

# Quantile connectedness across BRICS and international grain futures markets: Insights from the Russia-Ukraine conflict

Yan-Hong Yang<sup>a</sup>, Ying-Hui Shao<sup>b</sup>, Wei-Xing Zhou<sup>c,d,e,\*</sup>

<sup>a</sup>SILC Business School, Shanghai University, Shanghai 201899, China

<sup>b</sup>School of Statistics and Information, Shanghai University of International Business and Economics, Shanghai 201620, China

<sup>c</sup>School of Business, East China University of Science and Technology, Shanghai 200237, China

<sup>d</sup>Research Center for Econophysics, East China University of Science and Technology, Shanghai 200237, China

<sup>e</sup>School of Mathematics, East China University of Science and Technology, Shanghai 200237, China

---

## Abstract

This study examines the quantile connectedness among grain futures markets in BRICS and international markets, with a particular focus on the ongoing and escalating impacts of the Russia-Ukraine conflict. The findings reveal significant heterogeneity in spillover effects across different quantiles and market conditions. Specifically, the time-varying total connectedness index (TCI) consistently fluctuated around 95% under both extreme bearish and bullish market conditions, markedly higher than in normal market conditions. Moreover, across all quantile levels, the TCI was higher during the pre-outbreak period than in the post-outbreak period. This systemic risk has notably decreased following the onset of the Russia-Ukraine conflict and the subsequent changes to the Black Sea Grain Initiative. Apart from rice, U.S. grain futures maintained a dominant position as benchmarks for international grain prices, exerting substantial influence over the grain futures markets in BRICS throughout most of the period. Finally, the study highlights that the influence of grain type and regional proximity strengthens pairwise connectedness among futures markets, with short-term spillovers being dominant and the spillover effect generally symmetric across quantiles.

**Keywords:** Grain futures markets, Quantile connectedness, Russia-Ukraine conflict, Time-frequency, BRICS

---

## 1. Introduction

Food security is a fundamental basis for the healthy and stable development of socio-economic systems. In recent years, international grain prices have experienced several sharp fluctuations due to a confluence of factors including the COVID-19 pandemic, extreme weather events, economic shocks, trade frictions, and geopolitical conflicts (Zhou et al., 2024a). These fluctuations have dramatically increased the number of people suffering from poverty and hunger, placing unprecedented pressure on the global food supply chain. As reported in *The State of Food Security and Nutrition in the World 2023*<sup>1</sup>, the situation remains critical, with approximately 900 million people experiencing severe food insecurity in 2022.

Specifically, the ongoing Russia-Ukraine conflict, now entering its third year, has had profound impacts on the global food system (Naeem et al., 2024; Zhou et al., 2024b; Jiang and Chen, 2024; Cui and Maghyereh, 2024; Gao et al., 2022), resulting in hunger for approximately 23 million people. Russia and Ukraine are not only significant producers of food, energy, and fertilizers but also major exporters of wheat, barley, maize, and sunflower oil. In 2021, these two countries accounted for 14.3%, 19.0%, and 4.5% of the global production of wheat, barley, and maize, respectively. According to the Food and Agriculture Organization of the United Nations (FAO), by the end of 2021, the export shares of these two countries in the global market were notably high, with sunflower oil at 78.00% (Russia 28.00%, Ukraine 50.00%), wheat at 32.53% (Russia 21.99%, Ukraine 10.54%), barley at 29.60% (Russia

---

\*Corresponding author.

Email address: wxzhou@ecust.edu.cn (Wei-Xing Zhou)

<sup>1</sup><https://www.fao.org/publications/home/fao-flagship-publications>

12.93%, Ukraine 16.67%), and maize at 16.25% (Russia 2.25%, Ukraine 14.00%). The conflict has directly disrupted critical supply chains and export routes in these countries, leading to tensions and price fluctuations in the global food market, severely affecting the food security and economic stability of countries reliant on these imports (Behnassi and El Haiba, 2022). Furthermore, the conflict has exacerbated trade protectionism and export restrictions, driving up global food prices and causing serious concerns about food security in at least 50 countries and regions.

In July 2022, the Black Sea Grain Initiative was established<sup>2</sup>, which temporarily eased some tensions by stipulating safe humanitarian corridors for the export of food and fertilizers. However, due to disagreements, this initiative was suspended on 17 July 2023, once again impacting the global food supply. In the long term, the Russia-Ukraine conflict may prompt a reorganization of global agricultural trade patterns, with nations seeking greater self-sufficiency or developing new supply sources to reduce reliance on a single region and enhance resilience against future crises (Neik et al., 2023). The conflict not only exposes the high sensitivity and vulnerability of the global food security system to geopolitical events but also compels the international community to reconsider and strengthen food security strategies to address the continuously spreading and intensifying effects of the food crisis. This backdrop highlights the urgent need to thoroughly explore the dynamics of international grain markets, particularly focusing on how major grain-producing and consuming nations are interconnected, and how conflicts such as the Russia-Ukraine war impact these connectedness relationships.

The BRICS countries play a crucial role in stabilizing global grain supplies and prices, while the expansion of the new BRICS nations<sup>3</sup> has further amplified the group's influence in the global grain market. For instance, Brazil is a leading exporter of soybeans and corn, while India and China are major producers and consumers of various grains. Focusing on the BRICS nations allows for a deeper understanding of how changes in their agricultural output, trade policies, and economic conditions affect global grain markets and futures. Moreover, existing research on grain futures predominantly emphasizes developed countries or adopts a global perspective (Jiang and Chen, 2024; Zhu et al., 2024; Cui and Maghyereh, 2024; Naeem et al., 2024; Zhou et al., 2024b), with relatively limited attention to the entire BRICS group. As the BRICS has expanded from the original five members to the current ten, investigating the significance of agricultural futures markets in this newly formed BRICS framework has become increasingly critical, carrying both theoretical and practical implications.

The grain futures market, as a key price discovery mechanism, reflects market expectations for future grain supply and demand. Consequently, futures prices serve as critical indicators and reliable benchmarks for spot pricing (Zhou et al., 2024a). From the perspective of grain futures, the Russia-Ukraine conflict has significantly disrupted global grain supplies, leading to increased volatility in grain futures markets. This study investigates the quantile connectedness and spillover effects among grain futures markets of the BRICS nations and international grain markets (United States, Argentina, Ukraine, Black Sea), focusing on the impacts of the Russia-Ukraine conflict and the Black Sea Grain Initiative. Analyzing key commodities such as soybean, maize, wheat, and rice, we begin by characterizing their connectedness from both static and dynamic perspectives in the time domain, revealing how market interdependencies evolve under different market conditions before and after the conflict, while highlighting shifts in the roles of these commodities as transmitters and receivers of shocks. We then extend our investigation to the frequency domain, examining static and dynamic connectedness to capture the differences in spillover effects across various investment horizons. Utilizing the quantile vector autoregressive (QVAR) model (Baruník and Křehlík, 2018; Ando et al., 2022), we quantify these relationships along multiple dimensions, including the total connectedness index (TCI), directional spillovers (FROM and TO), net spillovers (NET), and net pairwise directional connectedness (NPDC). Additionally, we conduct a quantile sensitivity analysis to assess how connectedness varies across different quantiles, revealing insights into market behavior under both normal and extreme conditions, including an exploration of the approximate symmetry of spillovers across quantiles. Through this comprehensive approach, we aim to provide valuable insights for investors and policymakers in managing risks related to global food security, emphasizing the interconnectedness of soybean, maize, wheat, and rice futures markets and the importance of monitoring spillover effects during periods of geopolitical instability.

In summary, this study makes several contributions to the existing literature. First, to the best of our knowledge,

---

<sup>2</sup>For more detailed information, readers can refer to the official United Nations page on the Black Sea Grain Initiative: <https://www.un.org/en/black-sea-grain-initiative>.

<sup>3</sup>It should be noted that the original BRICS countries—Brazil, Russia, India, China, and South Africa—have recently been joined by five additional emerging nations: Egypt, Ethiopia, Iran, Saudi Arabia, and the United Arab Emirates, thus expanding the group to ten countries.

this study is the first to apply the quantile vector autoregressive model to examine the quantile connectedness between grain futures markets in the BRICS countries and international markets, including the U.S., Argentina, Ukraine, and the Black Sea region. By doing so, it provides new insights into how market dynamics vary under different market conditions, ranging from extreme bearish to bullish scenarios. Second, the study highlights the significant influence of geopolitical events, particularly the Russia-Ukraine conflict—which is ongoing and whose impact is escalating—on the systemic risk within global grain futures markets, offering empirical evidence of the changes in connectedness across various quantiles. Third, by focusing on the roles of grain type and regional proximity in strengthening pairwise connectedness, the study contributes to the understanding of how these factors drive the transmission of shocks across markets. Lastly, the research extends existing literature by incorporating time-varying and frequency-domain analyses, offering a more nuanced view of short-term versus long-term spillovers, especially in response to major global events. These contributions collectively advance our understanding of connectedness in grain futures markets and provide valuable implications for investors, policymakers, and researchers.

The study is organized as follows. Section 2 provides a review of the relevant literature. Section 3 presents the data sources along with the statistical descriptions. Section 4 describes the QVAR methodology employed. Section 5 offers the empirical analysis, and Section 6 concludes with a discussion of the key findings and their implications.

## 2. Literature review

The connectedness and spillover effects between commodity markets have always been a focus of attention, especially with the continuous financialization of commodities (Gong et al., 2023; Zhou et al., 2024a; Wei et al., 2023; Tiwari et al., 2022; Le et al., 2023; Zhang et al., 2023; Jiang and Chen, 2024; Zhu et al., 2024; Cui and Maghyereh, 2024; Naeem et al., 2024; Zhou et al., 2024b). Our study explores the changing characteristics of connectedness in the international grain futures markets and the impact of the Russia-Ukraine conflict on these dynamics. Therefore, we review the literature from three perspectives: the connectedness within grain futures, the connectedness between grain futures and other commodity futures markets, and the impact of the Russia-Ukraine conflict on the grain futures markets.

### 2.1. Connectedness within grain futures markets

The financialization of grain commodities underscores the importance of analyzing interdependencies among grain futures markets from the perspectives of connectedness or risk spillover (Ouyang and Zhang, 2020; Aït-Youcef, 2019; Just and Echaust, 2022; Hamadi et al., 2017; Wang et al., 2024; Zhu et al., 2024), which helps us better understand market responses under various economic scenarios, particularly in times of global economic turbulence. Ke et al. (2019) employ the CoVaR approach to study risk transmission between the U.S. and Chinese agricultural futures markets for soybean, corn, and sugar, revealing that soybean markets exhibit greater risk transmission than sugar and corn markets. Likewise, by utilizing the CoVaR family of methods, Hu et al. (2024) reveal significant and asymmetric extreme risk spillovers between the US and Chinese futures markets for soybean, wheat, and notably, corn, which uniquely shows no downside risk spillovers. Moreover, the dependence structure between these futures markets shifts markedly during periods of stability and crisis, with extreme risk spillover effects intensifying by major events such as the Global Financial Crisis, the COVID-19 pandemic, and the Russia-Ukraine conflict. Živkov et al. (2020) use an MS-GARCH model and Bayesian quantile regression to examine the volatility spillover effect among corn, wheat, soybean, and rice futures. The results indicate that soybean and wheat futures experience high volatility shocks from other markets, making them less ideal as primary investment assets. Conversely, rice futures receive the lowest volatility shocks, suggesting they are the most stable and suitable as a primary asset in a portfolio. Li and Hayes (2017) investigate the lead-lag relationships among soybean prices in U.S., Brazilian, and Chinese futures markets, finding that U.S. soybean futures lead long-term price changes in Brazil and China, while short-term price interactions exist primarily between U.S. overnight returns and Chinese No. 1 soybean futures. However, Han et al. (2013) employ Structural Vector Autoregressive and Vector Error Correction models to demonstrate that the Dalian Commodity Exchange (DCE) significantly contributes to global soybean futures price discovery, with bidirectional information transfer between DCE and the Chicago Board of Trade (CBOT), challenging the traditional view of DCE as a satellite market dominated by CBOT. Further, Jiang et al. (2017) confirm significant bidirectional volatility spillovers between U.S. and Chinese agricultural futures markets, particularly for soybean, wheat, and corn, with U.S.

short-term volatility impacting China and increasing evidence of Chinese market pricing power. [Jiang et al. \(2016\)](#) examine return spillovers of soybeans, wheat, corn, and sugar between U.S. and Chinese futures markets using a quantileogram, revealing significant bidirectional dependence, especially in extreme quantiles, with a moderately stronger influence from the U.S. to China, offering insights into market integration and efficiency. [Chen and Weng \(2018\)](#) adopt a VAR-BEKK-MGARCH model to examine mean and volatility spillovers, accounting for skewness, in U.S. and Chinese corn, wheat, and soybean futures, finding that the U.S. plays a major role in information transmission, while China's volatility spillovers to the U.S. increase in marketized commodities and post-trading structure changes

## 2.2. Connectedness between grain and other commodity futures markets

Compared to the relatively limited research on connectedness within grain futures markets, there is an extensive body of literature examining the connectedness between grain futures and other commodity futures markets ([Cui and Maghyereh, 2024](#); [Tiwari et al., 2022](#); [Kumar et al., 2021](#); [Rezitis et al., 2024](#); [Kang et al., 2017](#); [Zhang et al., 2023](#); [Xiao et al., 2020](#); [Yang et al., 2024](#)). Among these studies, the connectedness between grain commodity futures and energy commodity futures is the most extensively researched. The remaining literature includes, but is not limited to, studies on the connectedness between grain futures and precious metals futures markets.

Using the rolling window-based Quantile VAR model, [Tiwari et al. \(2022\)](#) examine the volatility spillovers between energy and agricultural markets, finding that corn, wheat, and soybean play significant roles in transmitting market volatility, with over 30% of their volatility attributed to network connections with other markets. The study reveals that these agricultural commodities are more closely linked to energy markets compared to natural gas, ethanol, and coffee, and that spillover effects are particularly pronounced under extreme market conditions. The COVID-19 pandemic has further intensified the volatility and interconnectedness between these markets. [Kumar et al. \(2021\)](#) explore the energy-food nexus using the dependence-switching copula model, focusing on grain commodities (corn, oats, soybeans, and wheat) and the WTI oil price across four market states. They found that oil and grain commodity crashes often coincide during crises but not in normal conditions, indicating that investors can't achieve excess profits in both markets simultaneously. Additionally, the return chasing effect was prevalent for all commodities, with significant risk spillover from oil to grain markets, particularly during the financial crisis. [Rezitis et al. \(2024\)](#) investigate the volatility linkages between energy and grain futures, revealing that external shocks have an asymmetric effect on the relationship of these assets, with higher cross-correlations during high volatility regimes. Using Markov-switching regressions and quadrivariate VAR-DCC-GARCH and VAR-BEKK-GARCH modeling, the research demonstrated that the comovement effect outweighs the substitution effect between WTI crude oil, natural gas, corn, and soybeans. Additionally, the quadrivariate VAR-BEKK-GARCH model confirmed a bidirectional price volatility spillover between agricultural and energy markets during high volatility periods.

[Kang et al. \(2017\)](#) analyze spillover effects among six commodity futures markets—gold, silver, WTI crude oil, corn, wheat, and rice—using the DECO-GARCH model and spillover index. Findings reveal that return correlations increased during the global financial and European sovereign debt crises, reducing the benefits of portfolio diversification. Bidirectional return and volatility spillovers were more pronounced post-crisis, indicating strong spillover impacts during crises. Gold and silver acted as information transmitters, while the other commodities were spillover receivers during financial stress periods. [Zhang et al. \(2023\)](#) introduce a network topology approach to discern both contemporaneous and noncontemporaneous idiosyncratic risk spillovers in commodity futures markets, demonstrating that contemporaneous information is more critical in constructing networks, particularly for higher-moment risks. Key findings indicate that gold, silver, and wheat are major transmitters of volatility and kurtosis risks, while corn and silver significantly transmit skewness risks. [Xiao et al. \(2020\)](#) find that metal futures act as net transmitters of shocks, while grain futures such as wheat and corn are particularly susceptible to these shocks. They discovered that nearly two-thirds of volatility uncertainty in commodity futures stems from interconnected shocks, with connectedness increasing notably during periods of market turmoil.

## 2.3. Impact of the Russia-Ukraine conflict on the grain futures markets

The Russia-Ukraine conflict has drawn substantial scholarly attention, particularly regarding its spillover effects and connectedness in global grain futures markets ([Zhou et al., 2024a](#); [Just and Echaust, 2022](#); [Wu et al., 2023](#); [Zhang et al., 2024](#); [Zhou et al., 2024b](#)). Researchers have extensively examined how this geopolitical tension has led to increased volatility, disrupted supply chains, and heightened market uncertainty, impacting global food security and economic stability ([Behnassi and El Haiba, 2022](#); [Jiang and Chen, 2024](#)).

Zhou et al. (2024a) propose a new analytical framework for tail dependence by integrating the Copula-CoVaR method with the ARMA-GARCH-skewed Student-t model. This framework analyzes the tail dependence structure and extreme risk spillover between agricultural futures and spot markets over the pre- and post-Russia-Ukraine conflict periods. Findings reveal that the tail dependence structures in soybean, maize, wheat, and rice markets have responded to the conflict. Moreover, the conflict has heightened risks in these markets, particularly wheat. Significant downside and upside risk spillovers to corresponding spot markets are detected, with notable asymmetries in directional (downside vs. upside) and temporal (pre- vs. post-outbreak) levels. Just and Echaust (2022) employ dynamic DY and BK spillover indices to reveal increased integration among agricultural commodity markets from the post-COVID-19 recovery phase to the Russia-Ukraine conflict. They underscore significant return spillover among key commodities such as wheat, maize, and barley, which are identified as the main transmitters of price shocks during the conflict. Additionally, their study emphasizes rising uncertainty in the global grain market and notes the isolation of the rice market from other agricultural commodities. Wu et al. (2023) adopt the TVP-VAR frequency connectedness method to evaluate the volatility connectedness induced by the COVID-19 pandemic and the Russia-Ukraine conflict, highlighting that the pandemic led to a more pronounced increase in connectedness, particularly through high-frequency and medium-frequency channels. Initially, fossil energy was the main risk transmitter, shifting risks primarily to energy crops like corn and soybean, while during the conflict, agricultural commodities, especially wheat and corn, emerged as the main transmitters. The paper underscores its novelty in exploring the volatility connectedness between these commodities across such global crises, revealing that the transmission of risks during the pandemic was mostly short-term to medium-term, whereas it extended beyond one month during the conflict. Zhang et al. (2024) investigate how global crises like the COVID-19 pandemic and the Russia-Ukraine war have impacted the U.S. and Chinese agricultural futures markets. Utilizing wavelet coherence analysis and time-varying parameter vector autoregression, they find that both events altered the correlation and lead-lag comovement between U.S. and Chinese soybean and corn futures returns, with minimal impact on cotton futures. U.S. markets transmit more volatility risk to Chinese markets than vice versa, and the war has a stronger risk spillover effect than the pandemic, especially in soybean and corn markets. Zhou et al. (2024b) examine the time-varying market linkages between energy and agricultural commodities during the COVID-19 pandemic and the 2022 Russia-Ukraine conflict. Using a novel time-varying parameter vector autoregressive model, they find asymmetry in volatility spillovers, with stronger effects across quantiles than at the mean. Crude oil is identified as the main transmitter of shocks, especially before the conflict, while both crude oil and natural gas transmit volatility in both periods. The conflict notably shifts numerous agricultural commodities from transmitters to receivers of volatility. Their analysis also reveals time-varying connectedness between crude oil and other commodities, with increased dependency on crude oil for major exports like wheat.

Existing empirical studies present mixed evidence on the nexus between grain and other commodity futures markets. However, the risk spillovers within BRICS nations and between BRICS and international grain markets, particularly during major geopolitical events, remain underexplored. Therefore, this study integrates time and frequency domain perspectives to thoroughly analyze the dynamic evolution of connectedness and risk transmission patterns between BRICS and international grain futures markets under varying market conditions, especially in the context of the Russia-Ukraine conflict.

### 3. Data and preliminary analysis

#### 3.1. Data description

We have selected various grains from BRICS countries, primarily focusing on commodities such as corn, soybeans, wheat, and rice. Considering that CBOT futures prices are a crucial reference and benchmark for the international pricing of agricultural commodities, we picked a range of grain futures from the CBOT to gauge international grain prices. We opted for commodity futures over spot market prices because futures are financial assets heavily influenced by market expectations, which facilitate better price discovery and enhanced liquidity (Shao et al., 2019; Yang and Shao, 2020). Unlike the spot market, which offers immediate purchase and delivery prices for commodities, futures contracts provide prices for the delivery of specified quantities of an underlying commodity at various maturities.

The dataset includes daily closing prices of continuous contracts from April 12, 2021, to August 11, 2023, totaling 610 observations. Missing data points were filled using the previous day's data, and if necessary, backfilled further

to maintain consistency and completeness. All the data were sourced from the Wind (<https://www.wind.com.cn>) and Bloomberg (<https://www.bloomberg.com>) databases. Additionally, to investigate the impact of the Russia-Ukraine conflict on the spillover effects of grain futures in BRICS countries, we divided the entire sample into two periods. The first period, referred to as the pre-outbreak period, covers the timeframe from April 12, 2021 to February 23, 2022. The second period, referred to as the post-outbreak period, spans from February 24, 2022 to August 11, 2023.

Due to limitations in data accessibility, we were unable to procure grain futures data for the Russian market. Therefore, we are considering using Black Sea wheat futures traded on the CBOT as a substitute for the Russian market. Simultaneously, as previously mentioned, Ukraine is also a significant global wheat exporter, with a substantial share in the international market. Additionally, Ukraine is one of the principal parties involved in the ongoing conflict. Hence, our analysis also includes Ukrainian wheat futures traded on the CBOT. However, impacted by the halt of the Black Sea Grain Initiative on July 17, 2023, CBOT has ceased trading and clearing of all futures and options of the Ukrainian Wheat (Platts), Black Sea Wheat Financially Settled (Platts), and Black Sea Corn Financially Settled (Platts) contracts, with this amendment to the listing schedule effective from August 16, 2023, as detailed in SER-9233<sup>4</sup>. Consequently, the cutoff date for the data sample was set to August 11, 2023. In addition, due to lack of data variability over the employed period, we decided to exclude the wheat futures in China from our analysis.

It should be noted that some of the new BRICS countries lack well-established grain futures contracts. Therefore, this study only includes the original BRICS countries. Furthermore, although Argentina was invited to join the new BRICS countries in 2023, President Javier Milei formally declined the offer on December 29, 2023. Considering Argentina's role as a major global exporter of corn and soybeans, we included Argentina's corn, soybean, and wheat futures in the grain data selection. Particularly, Argentina's MATBA-ROFEX, the largest agricultural futures and options exchange in South America, provides important grain futures that serve as key indicators of regional grain prices. Ultimately, 23 types of grain futures were extracted based on data availability and quality.

These 23 futures are sourced from various exchanges within BRICS countries and the CBOT exchange. They include cash-settled corn and mini soybean-CME futures contracts traded on Brazil's BMF exchange; maize and bajra futures contracts traded on India's NCDEX exchange; soybean, corn, and polished round-grained rice futures contracts traded on China's DCE exchange; white maize, yellow maize, corn-CBOT, soybean, soybean-CBOT, and wheat futures contracts traded on South Africa's SAFEX exchange; maize, soybean, and wheat futures contracts traded on Argentina's MATBA-ROFEX exchange; and Ukrainian wheat, Black Sea wheat, Santos Soybeans, soybean, corn, wheat, and rough rice futures contracts traded on the CBOT exchange. For the sake of simplicity in subsequent tables and figures, these 23 grain futures are abbreviated as BRc, BRms, INm, INb, CNs, CNC, CNr, ZAwM, ZAym, ZAc, ZAs, ZAcS, ZAw, ARm, ARs, ARw, UAw, BSw, BRs, USs, USc, USw, and USr, in the order mentioned previously. The abbreviations, with the first two uppercase letters representing the ISO-2 country codes, refer to the origin countries of the grain futures underlying assets. This study considers BRICS countries—Brazil, India, China, and South Africa—as well as other major global markets, including Argentina, Ukraine, the Black Sea region, and the United States, with the respective ISO-2 codes being BR, IN, CN, ZA, AR, UA, BS<sup>5</sup>, and US. Notably, there are two types of grain futures from BRICS countries: one type is traded on commodity exchanges within the BRICS countries, and the other type is traded on the CBOT, representing the underlying assets from the BRICS countries. As an illustration, the contract 'FOB Santos Soybeans' (BRs) refers to a soybean futures contract on the Chicago Board of Trade for soybeans to be delivered at the port of Santos in Brazil. Moreover, the corn-CBOT contract (ZAc) denotes a futures contract for corn traded on SAFEX and linked to CBOT. The explanations for soybean-CBOT (ZAcS) and soybean-CME (BRms) are similar.

### 3.2. Preliminary analysis

Table 1 reports the summary statistics and diagnostic test results of the return series for 23 grain futures over the entire sample period. The return series are calculated as the logarithmic returns of grain futures, defined as  $\ln(p_{i,t}/p_{i,t-1})$ , where  $p_{i,t}$  represents the daily closing price of the  $i$ -th grain futures at time  $t$ . As shown in Table 1,

---

<sup>4</sup>For detailed information, readers can refer to <https://www.cmegroup.com/notices/ser/2023/08/SER-9233.html>

<sup>5</sup>BS is the ISO-2 code for The Bahamas. The Black Sea region does not have a dedicated ISO code. In this study, we use BS to represent the Black Sea region for consistency.

among the different return series, USw has the highest standard deviation, whereas CNr has the lowest. Combining the results of skewness (Skew), kurtosis (Ex.Kurt), and the Jarque-Bera (JB) statistics, which found that all return series except for ZAs, ZAwM, and ZAym rejected the normality test at the 1% significance level, further supports the suitability of adopting the QVAR network connectivity approach. Moreover, the ADF and PP unit root tests indicate that all grain return series are stationary. Finally, the Ljung-Box Q statistic with lags of 20 reveals that, except for CNs and CNc, all other return series exhibit serial autocorrelation or conditional heteroskedasticity.

In the lower panel of Table 1, the non-parametric Kendall rank correlation coefficients between the returns of 23 grain futures are depicted. It can be observed that all statistically significant pairwise correlations are positive, indicating a synchronous trend among grain futures. Specifically, the maize (INm) and bajra (INb) futures contracts traded on India's NCDEX exchange and the polished round-grained rice (CNr) futures contracts traded on China's DCE exchange do not have a significant linear correlation with other grain futures.

Table 1: Summary statistics of the whole sample.

	BRms	BRs	CNs	ZAs	ZAs	ARs	USs	BRc	INm	CNs	ZAwM	ZAym	ZAc	ARm	USe	ZAw	ARw	Bsw	USw	Uaw	CNr	Usr	Inb
Mean	0.000	0.000	0.000	0.001	0.001	0.000	0.000	-0.001	0.001	0.000	0.000	0.001	0.000	0.000	0.000	0.001	0.000	0.000	0.000	0.000	0.000	0.001	
S.D.	0.014	0.013	0.010	0.013	0.016	0.013	0.016	0.013	0.016	0.008	0.016	0.009	0.017	0.025	0.009	0.019	0.012	0.026	0.013	0.004	0.015	0.014	
Skew	-0.530***	-0.627***	0.201**	-0.006	0.192*	-0.310***	-1.143***	0.184*	0.059	-0.471***	0.101	0.111	0.298***	-0.111	-1.936***	-0.033	0.142	0.498***	-0.403***	0.428***	2.666***	-1.569***	0.037
Ex.Kurt	3.952***	3.952***	3.952***	3.952***	3.952***	3.952***	3.952***	3.952***	3.952***	3.952***	3.952***	3.952***	3.952***	3.952***	3.952***	3.952***	3.952***	3.952***	3.952***	3.952***	3.952***	3.952***	
JB	419.470***	709.929***	599.247***	0.136	0.078*	243.852***	165.046***	127.755***	125.244***	91.758***	1.949	2.528	233.854***	123.096***	60.843***	70.299***	70.559***	3157.874***	406.963***	12137.676***	7300.795***	174.509***	
ADF	-8.177***	-8.011***	-7.210***	-7.728***	-9.020***	-7.494***	-7.494***	-7.783***	-7.837***	-8.402***	-8.623***	-7.398***	-7.839***	-8.423***	-7.873***	-6.539***	-7.809***	-6.601***	-8.684***	-9.339***	-6.511***		
PP	-51.472***	-488.658***	-509.923***	-506.981***	-551.992***	-543.662***	-594.476***	-721.725***	-598.664***	-591.665***	-573.610***	-585.177***	-474.710***	-567.868***	-651.851***	-599.568***	-631.183***	-538.272***	-467.558***	-621.027***			
Q(20)	24.188***	24.410***	7.571	27.527***	27.112***	11.547	17.443***	27.069***	16.462*	10.423	9.424	14.710	13.112	16.906*	16.307*	40.448*	23.088***	12.809	21.173***	13.967	18.203***	34.688***	25.873***
Q'(20)	36.411***	62.553***	10.99	27.042***	57.510***	74.116***	25.720***	165.388***	75.053***	4.263	40.613***	83.120***	82.757***	15.037	86.444***	84.774***	199.646***	133.106***	105.260***	1.909	25.304***	82.140***	
Kendall's $\rho$	BRms	BRs	CNs	ZAs	ZAs	ARs	USs	BRc	INm	CNs	ZAwM	ZAym	ZAc	ARm	USe	ZAw	ARw	Bsw	USw	Uaw	CNr	Usr	Inb
BRms	1.000***	0.728***	0.041	0.130***	0.152***	0.488***	0.666***	0.131***	0.018	0.062***	0.094***	0.101***	0.125***	0.303***	0.343***	0.032	0.263***	0.210***	0.287***	0.181***	-0.033	0.119***	-0.005
BRs	0.728***	1.000***	0.035	0.113***	0.131***	0.427***	0.618***	0.127***	0.022	0.072***	0.089***	0.114***	0.126***	0.299***	0.333***	0.022	0.239***	0.205***	0.260***	0.174***	-0.024	0.113***	-0.010
CNs	0.041	0.035	1.000***	0.085***	0.085***	0.056***	0.050	0.019	0.038	0.126***	0.062***	0.054***	0.038	0.003	0.004	0.007	0.044	0.025	0.036	0.044	0.027	0.010	
ZAs	0.130***	0.113***	0.085***	1.000***	0.552***	0.095***	0.092***	0.085***	-0.011	0.138***	0.434***	0.450***	0.455***	0.095***	0.052	0.251***	0.130***	0.106***	0.093***	0.085***	-0.009	0.060***	0.004
ZAc	0.152***	0.131***	0.080***	0.552***	1.000***	0.104***	0.117***	0.093***	-0.006	0.109***	0.427***	0.454***	0.508***	0.108***	0.055***	0.277***	0.094***	0.097***	0.086***	0.009	0.056	0.011	
ARs	0.488***	0.427***	0.056***	0.095***	0.104***	1.000***	0.474***	0.143***	0.164	0.060***	0.061***	0.078***	0.078***	0.315***	0.223***	0.029	0.243***	0.183***	0.209***	0.165***	0.019	0.069***	0.006
USs	0.048***	0.048***	0.092***	0.092***	0.092***	0.074***	1.000***	0.114***	0.017	0.060***	0.060***	0.060***	0.060***	0.060***	0.060***	0.029	0.174***	0.174***	0.174***	0.174***	0.174***	0.174***	
BRc	0.131***	0.127***	0.019	0.083***	0.093***	0.145***	0.114***	1.000***	0.010	0.059***	0.112***	0.113***	0.116***	0.231***	0.227***	0.089***	0.132***	0.099***	0.156***	0.123***	0.033	0.068***	0.002
INm	0.018	0.022	0.038	-0.011	-0.008	-0.014	0.017	0.010	1.000***	-0.050	-0.026	-0.029	-0.036	0.028	0.003	0.023	0.016	0.032	0.022	-0.012	-0.008	0.005	
CNs	0.062***	0.073***	0.126***	0.138***	0.109***	0.068***	0.060***	0.059***	-0.050	1.000***	0.136***	0.138***	0.148***	0.061***	0.016	0.096***	0.064***	0.067***	0.065***	0.025	-0.001	0.007	
ZAwM	0.094***	0.080***	0.062***	0.043***	0.427***	0.061***	0.045	0.112***	-0.026	0.136***	1.000***	0.846***	0.611***	0.128***	0.070***	0.323***	0.152***	0.119***	0.120***	0.106***	0.007	0.064***	0.014
ZAym	0.101***	0.088***	0.054***	0.054***	0.450***	0.454***	0.065***	0.052	0.113***	-0.029	0.138***	0.098***	0.668***	0.585***	0.109***	0.066***	0.346***	0.152***	0.124***	0.106***	0.004	0.068***	0.014
ZAc	0.125***	0.114***	0.038	0.045***	0.508***	0.078***	0.067***	0.116***	-0.036	0.148***	0.611***	0.668***	1.000***	0.148***	0.102***	0.381***	0.168***	0.163***	0.157***	0.141***	0.016	0.036***	-0.013
ARm	0.350***	0.299***	0.003	0.095***	0.108***	0.315***	0.293***	0.021***	0.005	0.061***	0.128***	0.139***	0.140***	1.000***	0.100***	0.078***	0.342***	0.281***	0.331***	0.257***	0.017	0.128***	-0.016
USe	0.343***	0.333***	-0.004	0.056***	0.223***	0.356***	0.228***	0.028	0.016	0.046***	0.102***	0.328***	1.000***	0.060***	0.028***	0.328***	0.286***	0.286***	0.286***	0.286***	0.286***	0.286***	
ZAw	0.251***	0.251***	0.007	0.056***	0.056***	0.056***	0.056***	0.056***	0.056***	0.056***	0.056***	0.056***	0.056***	0.056***	0.056***	0.056***	0.056***	0.056***	0.056***	0.056***	0.056***	0.056***	
ABw	0.263***	0.239***	0.044	0.030***	0.034***	0.245***	0.132***	0.023	0.064***	0.152***	0.152***	0.168***	0.342***	0.301***	0.129***	0.100***	0.381***	0.411***	0.341***	0.038	0.194***	0.009	
BSw	0.210***	0.205***	0.017	0.106***	0.108***	0.183***	0.178***	0.099***	0.016	0.067***	0.119***	0.125***	0.163***	0.281***	0.284***	0.131***	1.000***	0.435***	0.686***	-0.017	0.068***	0.021	
Usw	0.287***	0.260***	0.025	0.093***	0.097***	0.200***	0.156***	0.032	0.067***	0.120***	0.124***	0.157***	0.321***	0.384***	0.102***	0.411***	0.435***	1.000***	0.399***	-0.022	0.133***	-0.024	
Uaw	0.181***	0.174***	0.036	0.085***	0.086***	0.165***	0.146***	0.122***	0.022	0.065***	0.106***	0.141***	0.257***	0.239***	0.118***	0.341***	0.686***	0.399***	1.000***	-0.025	0.055	0.035	
CNr	-0.033	-0.024	0.044	-0.009	0.009	0.019	-0.017	0.033	-0.012	0.025	0.007	0.004	0.016	0.017	0.013	0.001	0.018	-0.022	-0.025	1.000***	-0.010	0.013	
USR	0.119***	0.113***	0.027	0.060***	0.056	0.096***	0.134***	0.068***	-0.008	-0.001	0.064***	0.068***	0.128***	0.135***	0.079***	0.119***	0.068***	0.133***	0.055	-0.010	1.000***	0.013	
INb	-0.005	-0.010	0.010	0.004	0.011	0.006	0.015	0.002	0.005	0.007	0.014	0.014	-0.013	-0.016	-0.046	0.009	0.009	0.009	0.009	0.013	0.013	1.000***	

Notes: JB represents the Jarque-Bera normality test statistic; ADF represents the Augmented Dickey-Fuller test statistic; PP represents the Phillips-Perron test statistic; Q(n) and Q'(n) represent the Ljung-Box Q statistic for testing autocorrelation and autocorrelation in the squared residuals up to lag  $n$ , respectively; \* indicates 10% significance level, \*\* indicates 5% significance level, \*\*\* indicates 1% significance level.

#### 4. Methodology

We utilize the quantile connectedness method proposed by Ando et al. (2022) and further elaborated upon by Chatziantoniou et al. (2021), to investigate the return risk spillover across quantiles in grain futures markets. As described by Chatziantoniou et al. (2021), the quantile-based vector autoregression model of lag order  $p$  and dimension  $n$  (QVAR( $p$ )) is estimated in the following manner:

$$\mathbf{y}_t = \boldsymbol{\mu}_t(\tau) + \boldsymbol{\phi}_1(\tau)\mathbf{y}_{t-1} + \boldsymbol{\phi}_2(\tau)\mathbf{y}_{t-2} + \cdots + \boldsymbol{\phi}_p(\tau)\mathbf{y}_{t-p} + \boldsymbol{u}_t(\tau) \quad (1)$$

where  $\mathbf{y}_t$  and  $\mathbf{y}_{t-i}$ ,  $i = 1, \dots, p$  are  $n \times 1$  dimensional endogenous variable vectors,  $\tau$  signifies the quantile level and ranges between 0 and 1,  $\boldsymbol{\mu}_t(\tau)$  is an  $n \times 1$  dimensional conditional mean vector,  $\boldsymbol{\phi}_i(\tau)$  is an  $n \times n$  dimensional QVAR

coefficient matrix, and  $\mathbf{u}_t(\tau)$  represents an  $n \times 1$  dimensional error vector associated with an  $n \times n$  dimensional variance-covariance matrix,  $\Sigma(\tau)$ . Utilizing Wold's theorem, the quantile vector moving average representation of infinite order, QVMA( $\infty$ ), for the QVAR( $p$ ) is given by:

$$\mathbf{y}_t = \boldsymbol{\mu}(\tau) + \sum_{j=1}^p \boldsymbol{\phi}_j(\tau) \mathbf{y}_{t-j} + \mathbf{u}_t(\tau) = \boldsymbol{\mu}(\tau) + \sum_{i=0}^{\infty} \boldsymbol{\psi}_i(\tau) \mathbf{u}_{t-i}. \quad (2)$$

Then the  $H$ -step Generalized Forecast Error Variance Decomposition (GFEVD) is conducted, which serves as a cornerstone of the connectedness analysis. The GFEVD reflects the proportion of the forecast error variance of a series  $i$  that can be attributed to shocks in series  $j$ , formulated as follows:

$$\theta_{ij}(H) = \frac{(\Sigma(\tau))_{jj}^{-1} \sum_{h=0}^H ((\boldsymbol{\psi}_h(\tau) \Sigma(\tau))_{ij})^2}{\sum_{h=0}^H (\boldsymbol{\psi}_h(\tau) \Sigma(\tau) \boldsymbol{\psi}'_h(\tau))_{ii}} \quad (3)$$

For comparability purposes, the decomposition values  $\tilde{\theta}_{ij}(H)$  undergo normalization by their respective row sums:

$$\tilde{\theta}_{ij}(H) = \frac{\theta_{ij}(H)}{\sum_{j=1}^n \theta_{ij}(H)} \quad (4)$$

This adjustment ensures that the sum of influences for each series equals one, thus indicating the proportion of shocks in series  $i$  affecting all other series  $j$ :

$$\sum_{i=1}^n \tilde{\theta}_{ij}(H) = 1 \quad \text{and} \quad \sum_{j=1}^n \sum_{i=1}^n \tilde{\theta}_{ij}(H) = n \quad (5)$$

Through this normalized measure, the extent to which a shock in any series impacts the entire network is encapsulated, indicating the aggregate connectedness within the system. In a words,  $\tilde{\theta}_{ij}(H)$  measures the spillover level of series  $j$  to series  $i$  in the quantile time domain.

Building on the frameworks established by [Diebold and Yilmaz \(2014\)](#) and [Chatziantoniou et al. \(2021\)](#), we proceed to compute all quantile-based connectedness measures as follows:

$$NPDC_{ij,t}(H) = \tilde{\theta}_{ij,t}(H) - \tilde{\theta}_{ji,t}(H) \quad (6)$$

$$TO_{i,t}(H) = \sum_{j=1, j \neq i}^n \tilde{\theta}_{ji,t}(H) \quad (7)$$

$$FROM_{i,t}(H) = \sum_{j=1, j \neq i}^n \tilde{\theta}_{ij,t}(H) \quad (8)$$

$$NET_{i,t}(H) = TO_{i,t}(H) - FROM_{i,t}(H) \quad (9)$$

$$TCI_i(H) = n^{-1} \sum_{i=1}^n TO_{i,t}(H) = n^{-1} \sum_{i=1}^n FROM_{i,t}(H) \quad (10)$$

where  $NPDC_{ij,t}$  represents the net pairwise directional connectedness between series  $i$  and  $j$  at time  $t$ , indicating the difference in influence exerted by series  $j$  on series  $i$  and vice versa, with positive values suggesting a dominant directional influence of series  $j$  over series  $i$ .  $TO_{i,t}(H)$  is the total directional connectedness to others, quantifying the aggregate influence transmitted by series  $i$  to all other series in the network at time  $t$ . Conversely,  $FROM_{i,t}(H)$  measures the total directional connectedness from others, encapsulating the cumulative influence received by series  $i$  from all other series.  $NET_{i,t}(H)$  delineates the net total directional connectedness, essentially the balance of influences, with positive values denoting a net transmitter of shocks or influence and negative values signifying a net receiver in the network structure. Lastly,  $TCI_i(H)$  denotes the total connectedness index at time  $t$ , reflecting the average degree

of interconnectivity and the systemic risk within the network, with higher values indicating greater overall market risk and interdependence.

We have previously concentrated on the time domain for analyzing connectedness and now move to comparable studies in the frequency domain. Employing the spectral representation of variance decompositions, as proposed by [Baruník and Křehlík \(2018\)](#), we delve into the frequency-based relationships in connectedness. We start with the frequency response function  $\psi(e^{-i\omega})$ , and from there, define the spectral density of series  $y_t$  at frequency  $\omega$ . This is captured by a Fourier transform of the QVMA( $\infty$ ) representation:

$$S_y(\omega) = \sum_{h=-\infty}^{\infty} E(y_t y'_{t-h}) e^{-i\omega h} = \psi(e^{-i\omega h}) \Sigma_t \psi'(e^{i\omega h}), \quad (11)$$

Significantly, the frequency-based generalized forecast error variance decomposition integrates spectral density with GFEVD. Like in the time domain, it's essential to normalize the frequency GFEVD. The normalization procedure is outlined as follows:

$$\theta_{ij}(\omega) = \frac{(\Sigma(\tau))_{jj}^{-1} |\sum_{h=0}^{\infty} (\psi(\tau)(e^{-i\omega h}) \Sigma(\tau))_{ij}|^2}{\sum_{h=0}^{\infty} (\psi(e^{-i\omega h}) \Sigma(\tau) \psi(\tau)(e^{i\omega h}))_{ii}} \quad (12)$$

$$\tilde{\theta}_{ij}(\omega) = \frac{\theta_{ij}(\omega)}{\sum_{j=1}^n \theta_{ij}(\omega)} \quad (13)$$

where  $\tilde{\theta}_{ij}(\omega)$  captures the influence of a shock in the  $j$ th series on the spectrum of the  $i$ th series at frequency  $\omega$ , serving as a within-frequency marker. To gauge connectedness across various timeframes, we integrate over the frequency spectrum,  $\tilde{\theta}_{ij}(d) = \int_a^b \tilde{\theta}_{ij}(\omega) d\omega$ , within a certain frequency ranges defined as  $d = (a, b)$ :  $a, b \in (-\pi, \pi)$ ,  $a < b$ , allowing us to compute connectedness measures the same as [Diebold and Yilmaz \(2014\)](#)'s metrics:

$$NPDC_{ij,t}(d) = \tilde{\theta}_{ij,t}(d) - \tilde{\theta}_{ji,t}(d) \quad (14)$$

$$TO_{i,t}(d) = \sum_{j=1, j \neq i}^n \tilde{\theta}_{ji,t}(d) \quad (15)$$

$$FROM_{i,t}(d) = \sum_{j=1, j \neq i}^n \tilde{\theta}_{ij,t}(d) \quad (16)$$

$$NET_{i,t}(d) = TO_{i,t}(d) - FROM_{i,t}(d) \quad (17)$$

$$TCI_t(d) = n^{-1} \sum_{i=1}^n TO_{i,t}(d) = n^{-1} \sum_{i=1}^n FROM_{i,t}(d) \quad (18)$$

These measures offer a detailed assessment of the directional and total connectedness within the given frequency band  $d = (a, b)$ , advancing our comprehension of the intricate interactions in grain futures markets. In line with the categorizations by [Gong et al. \(2023\)](#), this study identifies three frequency bands that correspond to distinct investment horizons. The high-frequency band,  $d_1 = (\pi/5, \pi)$ , covers the short-term range of 1–5 days. The mid-frequency band,  $d_2 = (\pi/20, \pi/5)$ , represents medium-term investment horizons of 5–20 days. Finally, the low-frequency band,  $d_3 = (0, \pi/20)$ , captures the long-term horizon of over 20 days.

Correspondingly, the metrics  $NPDC_{ij}(d_1)$ ,  $TO_i(d_1)$ ,  $FROM_i(d_1)$ ,  $NET_i(d_1)$ , and  $TCI(d_1)$  reflect the short-term connectedness;  $NPDC_{ij}(d_2)$ ,  $TO_i(d_2)$ ,  $FROM_i(d_2)$ ,  $NET_i(d_2)$ , and  $TCI(d_2)$  capture the medium-term connectedness; and similarly,  $NPDC_{ij}(d_3)$ ,  $TO_i(d_3)$ ,  $FROM_i(d_3)$ ,  $NET_i(d_3)$ , and  $TCI(d_3)$  delineate the long-term connectedness between series over these specified durations. Ultimately, we demonstrate how the frequency-domain metrics proposed by [Baruník and Křehlík \(2018\)](#) align with the time-domain measures outlined by [Diebold and Yilmaz \(2014\)](#):  $NPDC_{ij}(H) = \sum_d NPDC_{ij}(d)$ ,  $TO_i(H) = \sum_d TO_i(d)$ ,  $FROM_i(H) = \sum_d FROM_i(d)$ ,  $NET_i(H) = \sum_d NET_i(d)$ ,  $TCI(H) = \sum_d TCI(d)$ . Following the parameter setting of [Chatziantoniou et al. \(2021\)](#), we use a QVAR model with a rolling window period of 200 days, a lag length of 1 as determined by the Bayesian information criterion (BIC), and a forecast horizon of 20 steps.

Table 2: Average dynamic connectedness in the time domain at three different quantile levels (quantile = 0.5, 0.05, and 0.95 respectively) during the entire sample period.

	BRms	BRs	CNs	ZAs	ZAcS	ARs	USs	BRc	INm	CNc	ZAwM	ZAym	ZAc	ARM	USc	ZAw	ARw	BSw	Usw	Uaw	CNr	Usr	InB	FROM	
<i>Panel A: Lower quantile (<math>\tau=0.05</math>)</i>																									
BRms	5.86	5.09	4.10	4.10	3.98	4.52	4.97	4.58	4.47	4.50	4.19	4.13	3.88	4.80	4.07	4.07	4.34	4.08	3.90	4.30	3.68	3.94	4.46	94.14	
BRs	5.32	5.52	4.11	4.12	3.91	4.56	4.83	4.73	4.41	4.33	4.09	4.01	3.88	4.73	4.08	4.10	4.53	4.13	4.02	4.34	3.78	3.97	4.48	94.48	
CNs	4.80	4.69	5.33	4.06	4.04	4.56	4.68	4.74	4.52	4.29	4.21	4.16	4.07	4.61	3.84	4.10	4.47	4.23	3.83	4.36	3.84	3.96	4.61	94.67	
ZAs	5.25	4.93	4.09	4.96	4.20	4.74	5.05	4.68	4.01	4.01	4.18	4.18	4.23	4.77	3.91	4.14	4.38	4.26	3.87	4.34	3.64	3.86	4.32	95.04	
ZAcS	4.98	4.65	4.25	4.25	4.72	4.42	4.68	4.61	4.61	4.30	4.40	4.37	4.26	4.62	3.84	4.19	4.41	4.02	3.80	4.42	3.77	3.85	4.59	95.28	
ARs	5.21	4.86	4.18	4.10	3.98	5.56	4.84	4.75	4.39	4.33	4.05	3.94	3.89	4.83	3.98	3.98	4.60	4.26	3.95	4.28	3.72	3.93	4.38	94.44	
USS	5.16	4.81	4.18	4.09	4.02	4.62	5.46	4.64	4.57	4.50	4.17	4.06	3.82	4.67	4.09	4.05	4.53	4.12	3.94	4.44	3.63	4.07	4.37	94.54	
BRc	4.97	4.66	4.12	4.19	3.94	4.55	4.67	4.57	4.55	4.16	4.17	4.13	3.93	4.77	4.04	4.08	4.55	4.00	3.90	4.53	3.78	4.02	4.61	94.33	
INm	4.72	4.52	4.33	4.09	4.13	4.15	4.49	4.85	5.96	4.42	4.29	4.22	4.02	4.52	3.84	4.25	4.43	4.04	3.92	4.41	3.79	3.90	4.69	94.04	
CNc	4.68	4.46	4.37	4.00	4.07	4.35	4.50	4.64	4.53	4.54	4.31	4.22	4.02	4.62	4.05	4.13	4.54	4.17	3.88	3.85	4.54	4.44	3.85	94.46	
ZAwM	4.63	4.35	4.09	4.23	4.23	4.45	4.56	4.78	4.42	4.31	4.88	4.73	4.42	4.60	4.14	4.25	4.49	4.02	3.97	4.48	3.66	3.83	4.49	95.12	
ZAym	4.78	4.56	3.92	4.39	4.14	4.49	4.63	4.70	3.95	4.19	4.77	4.83	4.51	4.73	4.17	4.24	4.47	4.16	3.97	4.53	3.67	3.85	4.33	95.17	
ZAc	5.04	4.77	3.99	4.34	4.23	4.47	4.73	4.59	4.16	4.19	4.56	4.53	4.76	4.76	3.93	4.21	4.39	4.21	3.85	4.45	3.70	3.89	4.25	95.24	
ARm	5.17	4.87	4.01	4.09	3.91	4.77	4.79	4.74	4.21	4.20	4.10	4.02	4.08	5.68	3.97	4.08	4.74	4.23	4.08	4.30	3.68	3.90	4.36	94.32	
USe	5.11	4.75	4.11	4.07	4.02	4.35	4.74	4.62	4.41	4.36	4.26	4.24	4.09	4.00	4.66	5.00	4.23	4.43	4.20	3.96	4.51	3.81	4.00	4.35	95.00
ZAw	5.03	4.70	4.01	4.39	4.04	4.42	4.59	4.60	4.17	4.18	4.41	4.37	4.11	4.68	3.82	5.04	4.66	4.25	4.03	4.46	3.63	3.90	4.52	94.96	
ARw	4.88	4.59	4.14	4.00	3.97	4.53	4.50	4.87	4.51	4.29	4.20	4.13	3.95	4.82	4.02	4.16	5.35	4.18	4.13	4.53	3.68	3.95	4.58	94.65	
BSw	4.93	4.63	4.00	4.12	3.98	4.47	4.48	4.66	4.35	4.16	4.22	4.17	4.15	4.75	3.88	4.22	4.54	5.10	4.17	4.86	3.60	4.00	4.54	94.90	
Usw	4.80	4.57	4.19	4.00	4.05	4.38	4.55	4.61	4.61	4.54	4.30	4.21	4.00	4.73	3.88	4.15	4.74	4.32	3.61	4.03	4.40	4.95	3.61	95.21	
Uaw	4.74	4.49	4.22	4.15	4.04	4.40	4.49	4.61	4.50	4.40	4.30	4.06	4.15	4.65	4.00	4.17	4.57	4.65	4.07	5.34	3.67	3.90	4.46	94.66	
CNr	4.85	4.67	4.15	4.16	4.05	4.40	4.56	4.59	4.65	4.65	4.24	4.09	3.92	4.55	3.83	4.00	4.35	4.01	3.74	4.39	5.58	4.03	4.52	94.42	
USR	4.88	4.60	4.10	4.07	3.94	4.42	4.51	4.84	4.51	4.29	4.26	4.25	3.99	4.62	3.93	4.29	4.53	4.11	4.04	4.38	3.76	4.09	4.58	94.91	
INb	4.74	4.56	4.42	4.08	4.03	4.27	4.47	4.63	4.73	4.33	4.27	4.14	4.01	4.50	3.81	4.21	4.45	4.16	3.86	4.39	3.93	4.01	6.01	93.99	
TO	106.88	102.92	91.09	91.18	89.90	98.29	102.32	103.06	97.25	94.91	93.92	92.21	89.28	103.02	107.11	91.30	99.11	91.82	86.86	97.71	81.88	86.70	98.40	2177.95	
Inc.Own	114.54	108.45	96.92	96.14	93.62	103.85	107.78	108.73	103.21	100.46	98.79	97.04	94.05	108.70	92.11	96.35	104.47	96.92	91.65	103.05	87.47	91.79	104.42	TCI	
NET	14.54	8.45	-3.58	-3.86	-6.38	3.85	7.78	8.73	3.21	0.46	-1.21	-2.96	-5.95	8.70	-7.89	-3.65	4.47	-3.08	-8.35	3.05	-12.53	-8.21	4.42	94.69	
NPT	22.00	19.00	7.00	11.00	4.00	14.00	19.00	19.00	15.00	8.00	10.00	10.00	6.00	19.00	2.00	8.00	16.00	10.00	3.00	13.00	0.00	2.00	16.00		
<i>Panel B: Median quantile (<math>\tau=0.50</math>)</i>																									
BRms	28.49	17.42	0.17	0.51	0.65	10.44	15.37	1.81	0.52	0.90	0.64	0.55	0.92	6.70	3.57	0.23	3.18	1.88	2.62	1.76	0.12	1.01	0.35	71.51	
BRs	18.73	33.02	0.21	0.29	0.45	8.70	14.21	1.57	0.87	0.86	0.40	0.41	0.74	5.08	3.50	0.13	2.26	2.26	2.26	2.26	2.14	0.24	1.37	0.31	66.98
CNs	2.38	1.81	69.36	0.78	1.59	1.12	3.06	1.12	0.97	1.50	0.90	0.95	1.81	1.03	1.59	0.55	1.22	2.13	1.33	2.00	0.89	1.31	0.62	30.64	
ZAs	8.52	6.81	0.35	22.60	7.65	5.96	8.54	2.30	0.34	1.58	5.47	5.85	5.97	4.05	2.44	2.83	1.76	1.97	1.55	1.90	1.23	1.11	0.24	77.40	
ZAcS	8.88	7.60	0.49	7.13	22.56	4.71	6.76	1.43	0.57	1.02	5.38	6.09	9.21	4.48	2.04	3.17	1.65	1.62	1.63	0.46	1.22	0.21	77.44		
ARs	12.01	9.44	0.41	0.53	0.66	34.72	106.38	2.30	0.72	0.75	0.46	0.34	0.71	9.29	2.88	0.31	5.26	2.08	2.92	1.84	0.30	0.96	0.43	65.28	
USS	17.50	15.20	0.37	0.67	1.31	10.54	32.64	1.27	0.54	1.16	0.57	0.43	0.42	4.38	4.19	0.32	1.96	1.58	1.91	1.20	0.47	1.01	0.35	67.36	
BRc	3.49	2.72	0.56	1.13	1.20	3.43	2.11	51.55	2.01	1.00	1.86	2.53	7.45	3.79	0.78	4.35	1.10	2.85	1.81	0.60	1.13	0.55	48.45		
INm	0.96	1.67	0.35	0.52	0.37	0.33	0.97	1.72	84.55	0.68	0.60	0.37	0.68	0.24	0.33	0.97	0.55	0.18	0.47	0.61	0.74	1.35	0.54	15.46	
CNc	2.73	2.92	1.08	2.25	1.35	2.05	2.05	2.03	0.79	57.00	1.76	1.93	2.41	3.87	3.31	0.90	2.46	2.08	2.75	2.25	2.25	2.25	2.25	43.00	
ZAwM	2.06	1.72	0.20	5.66	5.66	1.90	1.85	2.20	0.32	0.82	24.51	21.09	10.91	2.90	4.30	2.27	7.73	5.20	5.02	0.37	1.71	0.27	64.21		
ZAym	2.19	2.16	1.09	5.53	6.01	1.90	1.93	2.33	0.36	0.84	19.38	22.50	12.13	3.38	4.80	4.85	1.95	1.80	2.01	2.47	0.28	0.76	0.25	77.50	
ZAc	2.68	2.43	0.23	5.61	8.99	2.02	1.87	2.71	0.34	1.26	9.81	12.08	22.69	4.45	5.09	5.35	2.69	2.83	2.73	2.72	0.32	0.89	0.23	77.31	
ARm	7.58	5.59	0.28	0.22	0.96	9.08	4.77	4.92	0.33	1.25	0.89	1.12	1.95	3.62	4.37	0.74	9.40	2.96	6.71	2.49	0.60	0.97	0.20	67.38	
USe	5.17	4.72	1.02	0.44	0.68	3.15	5.46	2.80	0.31	0.50	0.49	0.55	1.23	5.15	4.44	1.00	4.82	5.40	5.95	4.49	0.60	1.45	0.49	55.86	
ZAw	1.10	1.07	0.29	3.94	4.67	1.14	1.16	0.73	0.31	0.62	6.22	4.27	3.73	4.24	2.10	2.90	35.79	5.16	5.24	5.02	0.37	1.71	0.27	64.21	
ARw	3.85	2.75	0.18	0.23	0.58	5.66	2.28	2.64	0.72	0.55	1.19	1.01	1.74	10.40	3.88	1.36	36.27	6.88	9.97	5.7					

## 5. Empirical analysis

In this section, we utilize time-domain and frequency-domain connectedness methods to present the changes in long-term and short-term connectedness at different quantiles from both static (overall) and dynamic perspectives.

### 5.1. Static spillover effects of returns in grain futures markets

#### 5.1.1. Average dynamic connectedness measures in the time domain

Table 2 reports the average dynamic connectedness in the time domain at three different quantile levels during the entire sample period. No matter whether it is under normal market conditions (quantile = 0.5) or extreme market conditions (quantile = 0.05, 0.95), it can be observed that each variable contributes the most to its own forecast error variance, with the diagonal elements having higher values compared to the off-diagonal elements. However, the difference between the diagonal shocks and the off-diagonal shocks at the extreme quantiles of 0.05 and 0.95 is not as pronounced as under normal market conditions. Table 2 demonstrates that the interdependences among grain futures are more tightly connected under extreme market conditions, with the TCI reaching 94.69% and 95.24% at the 0.05 and 0.95 quantile levels, respectively, compared to 56.71% at the 0.5 quantile level under normal market conditions. In extreme bearish (quantile = 0.05) and extreme bullish (quantile = 0.95) market environments, both FROM-system and TO-system directional return connectedness are higher than in normal market conditions. Specifically, the FROM connectedness of each grain future clusters around 95%, and most TO connectedness values exceed 90%, with the lowest being ZAcs in the right-tail (quantile = 0.95) at 78.96%. When considering the median quantile, the five lowest TO spillovers are CNs (9%), INb (9.73%), CNr (10.49%), INm (13.89%), and CNC (19.09%), while the five lowest FROM spillovers are CNr (15.41%), INm (15.45%), INb (18.70%), CNs (30.64%), and USr (35.67%), indicating that the grain futures markets of China and India appear to be very weak participants in the information transmission mechanism under normal market conditions. This finding is consistent with the correlation characteristics between INm, INb, CNr, and other grain futures markets shown in Table 1.

Under extreme bearish market conditions, the CNr (-12.53%), USw (-8.35%), USr (-8.21%), USc (-7.89%), ZAcs (-6.38%), ZAc (-5.95%), ZAs (-3.86%), ZAw (-3.65%), CNs (-3.58%), BSw (-3.08%), ZAYm (-2.96%), and ZAwM (-1.21%) appear to be the main net receivers of shocks, whereas the major net transmitters of return shocks are BRMs (14.54%), BRc (8.73%), ARm (8.70%), BRs (8.45%), USs (7.78%), ZAw (4.47%), INb (4.42%), ARs (3.85%), INm (3.21%), UAw (3.05%), and CNC (0.46%). Notably, CNr has an NPT value of 0 at the 0.05 quantile, indicating zero net transmitted shocks. In extreme bullish market scenarios, grain futures such as ZAcs (-16.99%), INm (-11.91%), ZAc (-8.32%), USc (-8.16%), BRs (-7.39%), CNC (-6.52%), ZAw (-5.85%), INb (-5.04%), ZAs (-4.94%), BRMs (-2.68%), ZAYm (-1.69%), and ZAwM (-1.47%) predominantly absorb shocks. Conversely, grain futures like BSw (17.26%), UAw (14.49%), CNr (13.84%), ARw (6.90%), ARs (6.61%), USw (6.40%), USr (5.04%), ARm (4.46%), USs (3.27%), and CNs (2.78%) stand out as the principal distributors of shocks. When it comes to normal market conditions, ZAs (-37.69%), ZAcs (-29.51%), ZAw (-27.49%), CNC (-23.91%), CNs (-21.64%), ZAwM (-13.64%), USr (-11.87%), ZAYm (-10.07%), INb (-8.97%), BRc (-7.85%), ZAc (-6.79%), CNr (-4.91%), and INm (-1.56%) emerge as the main net recipients of shocks; while BRMs (40.36%), BRs (31.07%), ARm (25.44%), USs (24.88%), ARw (15.47%), USc (14.20%), BSw (13.09%), USw (13.07%), ARs (17.37%), and UAw (10.94%) serve as the main net transmitters of return shocks. Particularly, at the median-, lower-, and upper-quantiles, ZAs, ZAcs, ZAwM, ZAYm, ZAc, and ZAw all act as net receivers of shocks, while ARs, ARm, ARw, USs, and UAw play the role of net transmitters of shocks. It is evident that South African grain futures are primarily recipients of risk, whereas Argentine grain futures, U.S. soybean futures, and Ukrainian wheat futures are mainly sources of risk spillover. Overall, regardless of whether in the median, extreme lower, or extreme upper quantiles, futures of the same grain type exhibit stronger pairwise connectedness, as seen with wheat futures. Likewise, futures from the same region also show stronger connectedness. For instance, Black Sea and Ukrainian wheat futures display significantly higher pairwise connectedness than with other grain futures.

Table C.6 and Table C.7 provide the average dynamic connectedness in the time domain at different quantile levels before and after the Russia-Ukraine conflict, respectively. In normal market conditions, compared to the pre-outbreak TCI of 61.96%, the post-outbreak TCI dropped to 54.49%, indicating weaker interdependence among grain futures systems, while the left-tail or right-tail TCI remained comparable.

Additionally, in extreme bearish market conditions, net receivers of shocks in the pre-outbreak period included INm (-18.89%), INb (-18.46%), ZAc (-16.54%), USr (-11.36%), CNs (-10.20%), USw (-8.34%), BSw (-5.23%),

USc (-4.95%), ZAym (-3.99%), and CNc (-2.06%). In the post-outbreak period, they included USc (-11.92%), USr (-11.36%), CNr (-11.34%), USw (-9.84%), ZAym (-8.75%), BSw (-7.33%), ZAwm (-5.99%), CNs (-5.12%), ZAc (-4.65%), ZAw (-3.92%), ZAcs (-0.59%), and ARw (-0.36%). As for net transmitters of shocks, the pre-outbreak period identified ARw (13.17%), BRms (10.70%), UAw (9.78%), ARm (9.64%), ZAs (9.18%), USs (8.00%), BRc (7.68%), ARs (7.25%), ZAw (6.31%), ZAwm (5.56%), ZAcs (5.44%), BRs (3.83%), and CNr (3.50%), while the post-outbreak period identified BRms (24.64%), ARm (13.67%), BRc (9.41%), INb (8.26%), ARs (6.96%), BRs (6.41%), USs (4.19%), INm (4.20%), ZAs (2.82%), CNc (0.43%), and UAw (0.18%). The presence of several overlapping grain futures from the pre- to post-outbreak periods, such as USc, USr, USw, BSw, CNs, ZAym, and ZAc, highlights their persistent vulnerability and sensitivity to external shocks as net receivers of risk. In contrast, BRms, ARm, BRc, ARs, BRs, USs, ZAs, and UAw are net risk spillover transmitters in both the pre- and post-outbreak periods. Specifically, from the pre- to post-outbreak period, the shocks received by U.S. corn, wheat, and rice futures increased. The Indian grain futures market shifted from being a net receiver to a net transmitter, while Argentine wheat futures became net receivers of shocks. Brazilian soybean and corn futures consistently remained the primary net transmitters, with their transmission capacity growing to the strongest. Black Sea wheat futures consistently acted as net receivers, with the magnitude of shocks received increasing. Meanwhile, Ukrainian wheat futures, although consistently net transmitters, experienced a significant decrease in their transmission capacity, from 9.78% to 0.18%.

In the context of an extreme bullish market, over the pre-outbreak period, grain futures that were primary net receivers of shocks included INm (-30.41%), ZAw (-22.08%), ZAcs (-18.20%), USc (-12.92%), ZAc (-12.88%), CNs (-10.23%), BRms (-6.82%), BRs (-6.34%), USw (-3.62%), ARw (-1.20%), and BSw (-0.49%). The primary net transmitters of shocks to the system were UAw (49.92%), ARs (16.37%), ARm (12.73%), BRc (7.41%), CNr (8.61%), ZAs (6.84%), USr (6.76%), ZAwm (6.34%), USs (4.45%), ZAym (4.52%), CNc (1.25%), and INb (0.00%). During the post-outbreak period, primary net receivers of shocks were ZAcs (-16.77%), INb (-13.53%), BRs (-13.05%), USc (-11.10%), BRms (-9.72%), INm (-9.19%), ZAw (-8.81%), ZAc (-6.32%), ZAs (-5.00%), CNc (-4.84%), ARm (-4.47%), CNs (-2.77%), UAw (-0.67%), while the primary net transmitters were CNr (35.36%), USr (18.61%), ZAwm (18.21%), BSw (13.95%), ZAym (7.47%), BRc (7.07%), USw (4.57%), ARw (0.42%), USs (0.33%), ARs (0.26%). Clearly, regardless of the pre- or post-outbreak periods, INm, ZAw, ZAcs, USc, ZAc, CNs, BRms, and BRs consistently appear as net recipients of shocks, while ARs, BRc, CNr, USr, ZAwm, USs, and ZAym consistently act as net transmitters of shocks. In addition, unlike the left tail, in the right tail condition, Brazil's soybean and corn futures serve as net recipients of shocks in the pre-outbreak period. In comparison to the pre-outbreak period, the net receiver of shocks for Indian maize, South African wheat, South African soybeans, U.S. corn, South African maize, and Chinese soybeans has weakened post-outbreak. U.S., Argentine, and Black Sea wheat futures shifted from net receivers to net transmitters post-outbreak, with Black Sea wheat showing the most significant change from -0.49% to 13.95%, highlighting the impact of the Russia-Ukraine conflict. Conversely, South African soybeans and Chinese corn transitioned from net transmitters pre-conflict to net receivers post-conflict. It is particularly noteworthy that Ukraine, a direct participant in the Russia-Ukraine conflict, experienced a significant shift in the risk spillover direction of its wheat futures before and after the outbreak, moving from being the most dominant net transmitter (49.92%) during the pre-outbreak period to a net receiver (-0.67%) in the post-outbreak period.

Regarding the median quantile reported in Table C.6 and Table C.7, the information transmission mechanism differs somewhat from those observed in the lower and upper quantiles over the pre- and post-outbreak periods. During the pre-outbreak period, ZAcs (-42.16%), ZAs (-41.92%), ZAc (-35.85%), ZAw (-34.37%), ZAwm (-30.84%), CNc (-27.57%), ZAym (-25.34%), CNs (-23.52%), BRc (-11.97%), USr (-10.89%), CNr (-7.48%), INm (-7.07%), and INb (-4.45%) were the primary net receivers of shocks, while ARm (48.76%), USs (47.67%), BRms (46.91%), USc (31.79%), ARs (28.98%), BSw (28.32%), UAw (20.86%), BRs (20.09%), USw (20.06%), and ARw (9.99%) were the main net transmitters of shocks. Evidently, all grain futures in South Africa were the predominant risk absorbers, followed by China's corn, soybean, and rice futures, as well as Brazil's corn futures and U.S. rice futures, with the smallest being India's grain futures. Conversely, all grain futures in Argentina were chief net transmitters of shocks, with Argentine maize futures being the most dominant net transmitter, followed by U.S. soybean futures. Brazil's soybean futures were also major net transmitters of shocks. Additionally, the Black Sea wheat futures traded on the CBOT, Ukrainian wheat futures, Santos soybean futures, and U.S. soybean, corn, and wheat futures were all net transmitters. Correspondingly, ZAs (-33.26%), ZAcs (-30.51%), ZAw (-30.09%), CNc (-26.81%), CNs (-13.77%), INb (-11.52%), USr (-10.85%), ZAwm (-6.70%), CNr (-5.08%), ZAym (-3.40%), INm (-2.07%), ZAc (-1.87%), BRc (-1.29%), and USc (-0.71%) are the main net receivers of shocks over the post-outbreak period, while BRs (48.07%),

BRms (42.04%), ARm (24.33%), USw (19.15%), USs (18.32%), ARs (9.62%), ARw (9.41%), BSw (4.24%), and UAw (2.74%) are the primary net transmitters of shocks. Hence, under normal market conditions, the net transmitters and receivers during the two sample periods before and after the outbreak of conflict remain largely consistent, except for U.S. corn futures, which shifted from a net transmitter (31.79%) before the conflict to a net receiver (-0.71%) after the conflict. Naturally, the net spillover intensity of each grain futures differs between the pre- and post-conflict periods. Moreover, from the pre- to post-outbreak period, except for BRs, the net spillover intensity of all other transmitters significantly decreased, especially Black Sea wheat (28.32% to 4.24%) and Ukrainian wheat (20.86% to 2.74%), which became the weakest transmitters.

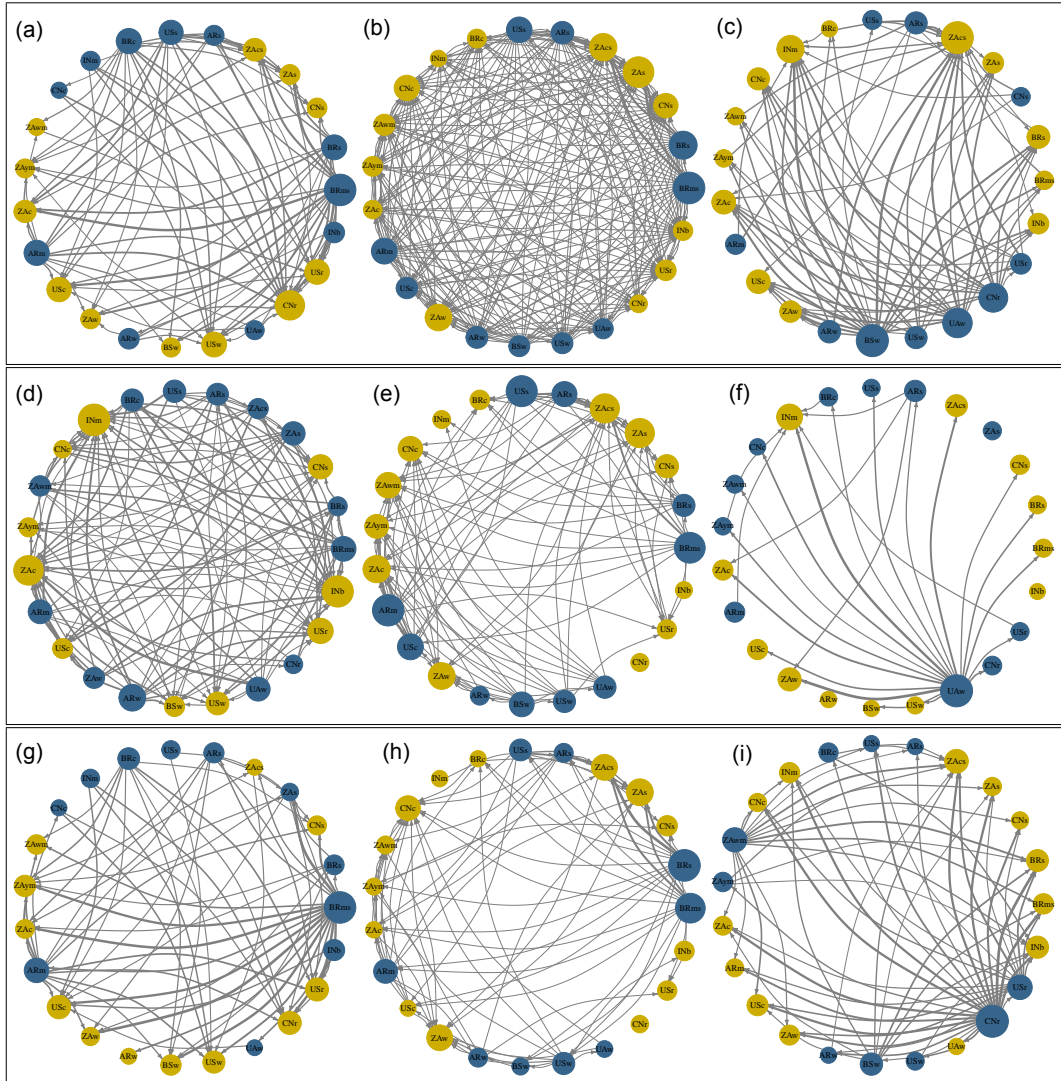


Figure 1: Network connectedness in the time domain. The upper, middle, and lower panels correspond to full sample, pre-outbreak, and post-outbreak samples, respectively. Specifically, (a), (d), and (g) represent the extreme lower quantile  $\tau = 0.05$ ; (b), (e), and (h) represent the median quantile  $\tau = 0.5$ ; and (c), (f), and (i) represent the extreme upper quantile  $\tau = 0.95$ . The node sizes depict the spillover effects from one grain futures contract to others. Additionally, the arrows' direction shows the flow of risk spillover (from transmitters to receivers), while the arrows' width, varying from slim to thick, indicates the intensity of risk spillover between grains futures.

To visually demonstrate the source, direction, and magnitude of spillovers, Fig. 1 shows the net pairwise connectedness network of the grain futures system at the 0.5, 0.05, and 0.95 quantile levels. Blue nodes indicate net transmitters of return shocks, while yellow nodes indicate net receivers. The size of each node reflects the magnitude

of weighted net total return connectedness, and the thickness of the edges represents the strength of pairwise spillover. It is evident from Fig. 1 that there is a consistent pattern with the findings of Ando et al. (2022) and Lei et al. (2024), showing that pairwise linkages among grain futures become tighter under extreme market shocks compared to normal market conditions. This is due to the more intense transmission of market information and convergence of investor behavior characteristics under extreme conditions (Ding et al., 2023). Fig. 1 further illustrates the role-switching characteristics between transmitters and receivers of various grain futures under different market conditions during the two subsample periods, before and after the outbreak of the Russia-Ukraine conflict. For instance, at the extreme high quantile level of 0.95, Ukrainian wheat shifted from being the largest transmitter of shocks over the pre-outbreak period to a net shock receiver during the post-outbreak period.

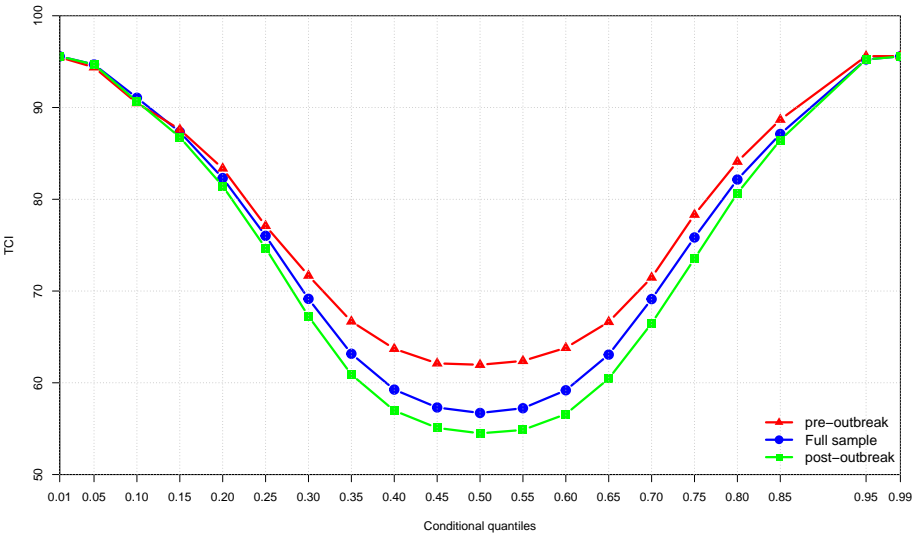


Figure 2: Varying TCI values across the quantiles for the three samples (full period, pre-outbreak, and post-outbreak). Notes: The results are based on a 200-day rolling window QVAR model with a lag length of 1 (BIC) and a 20-step-ahead GFEVD.

To further explore the impact of quantile selection on spillover effects, we plotted the TCI at different conditional quantiles for the full sample, pre-outbreak, and post-outbreak periods. As depicted in Fig. 2, we found that the spillover effects exhibit a distinct U-shaped pattern across the quantiles. Around the median quantile, the TCI is relatively low, but it rises sharply to nearly 95% at the upper and lower quantiles. Moreover, at all quantile levels, the TCI during the pre-outbreak period is higher than that over the post-outbreak period, and the difference between their TCIs grows larger as they approach the median quantile. The results in Fig. 2 once again demonstrate that the spillover effects among grain futures markets are more pronounced under extreme tail conditions, further validating our choice of the quantile VAR model.

### 5.1.2. Average dynamic connectedness measures in the frequency domain

After examining the static quantile connectedness in the time domain, we turn our attention to investigating static quantile connectedness in the frequency domain for BRICS and international grain commodity markets, with the results reported in Table 3. The short-term TCI at the lower, median, and upper quantiles are 75.16%, 46.85%, and 68.52%, respectively, indicating an extremely high level of connectedness among the grains. In contrast, the medium-term TCI is 9.30%, 6.56%, and 13.91%, while the long-term spillover strengths are 10.27%, 3.30%, and 12.82%. Clearly, the spillover strength decreases sharply from the short term to the medium term or long term. This finding is consistent with other studies, attributed to the rapid transmission of information in financial markets, leading to short-lived spillovers between assets (Le et al., 2023; Lei et al., 2024). Additionally, under normal market and extreme bullish market conditions, the TCI decreases progressively from the short term to the medium term and then to the long term. However, in an extreme bearish market, the long-term TCI is greater than the medium-term TCI. Pairwise connectedness also follows this pattern. Table C.8 shows that over the pre-outbreak period, the TCI or pairwise connectedness in the left tail is higher for the medium term than for the long term. Nevertheless, Table C.9 reveals

Table 3: Average dynamic connectedness in the frequency domain at three different quantile levels (quantile = 0.5, 0.05, and 0.95, respectively) during the entire sample period.

Notes: The connectedness table is derived from a quantile VAR model with a lag length of 1 (based on BIC) and a 20-step-ahead forecast. First and second values in parentheses represent medium- and long-term frequency connectedness measures, respectively, while all other values indicate short-term frequency connectedness. Each cell shows the spillovers from the grain listed in the top row to the grain listed in the first column. ‘FROM’ indicates the total directional return connectedness received from other grains. ‘TO’ denotes the directional return connectedness given to other grains. ‘Inc.Own’ represents the sum of the total directional connectedness of series  $i$  to all other series  $j$  and to itself. ‘NET’ is the net total directional return connectedness. ‘TCI’ reflects the overall spillover strength across the grains.

that during the post-outbreak period, the TCI, or pairwise connectedness at both tails, is lower for the medium term than for the long term. Overall, this indicates that the spillovers among grains are predominantly concentrated in the short run.

With respect to the NET spillovers in the left tail, Table 3 indicates that BRms, BRs, USs, ARm, ARw, and INm are net transmitters of shocks at short-, medium-, and long-term frequencies, while ZAc, ZAc, and USr are net receivers across all terms. USc, BSw, USw, UAw, CNr, and INb are receivers at the short-term frequency but transform into transmitters at the medium- and long-term frequencies. Conversely, ZAs, ARs, CNC, ZAwm, ZAym, and ZAw are transmitters at the short-term frequency but become receivers at the medium- and long-term frequencies. Among these grains, only INm, INb, and ARw exhibit significantly lower net spillover intensity in the short run compared to the medium and long term.

As for the right tail, BRms, BRs, ZAs, ZAc, INm, CNC, ZAc, and ZAw are consistently net receivers across all terms, while CNs, ARs, ARw, BSw, UAw, CNr, and USr are net transmitters. At the 0.5 quantile, BRms, BRs, ARs, USs, ARm, USc, ARw, BSw, USw, and UAw are net contributors of shocks across all three frequencies, while CNs, ZAs, ZAc, BRc, CNC, ZAwm, ZAym, ZAc, ZAw, CNr, and INb are net receivers. Notably, at the 0.5 quantile, with the exception of INm, the remaining grains exhibit consistent net spillover signs across short-, medium-, and long-term frequencies. However, at the extreme lower and upper quantiles, many grains transition between being receivers and transmitters across these frequencies. Therefore, there is heterogeneity in risk spillovers across short-, medium-, and long-term frequencies under different market conditions, with asymmetry observed between the right and left tails.

Taking a closer look at Table C.8 and Table C.9, it is observed that under extreme market conditions (at the 0.05 and 0.95 quantiles), the short-term TCIs are greater during the post-outbreak period compared to the pre-outbreak period, while the medium- and long-term TCIs are greater during the pre-outbreak period. Correspondingly, under normal market conditions, the short-, medium-, and long-term TCIs exhibit the opposite pattern compared to extreme market conditions.

In the left tail, USs, BRc, CNC, ZAw, UAw, and USr maintain consistent net spillover directions across short-, medium-, and long-term frequencies when comparing the pre-outbreak and post-outbreak periods, while in the right tail, BRms, BRs, CNs, ZAc, ZAym, USc, and ARw exhibit the same consistency in their NET signs. At the median quantile, except for INm, ZAc, USc, and UAw, the other grains show consistent net spillover directions across short-, medium-, and long-term frequencies between these periods. Overall, the Russia-Ukraine conflict significantly impacts risk spillovers in both tails, altering not only the direction but also the intensity of spillover effects across different frequencies.

Furthermore, the patterns of frequency domain connectedness presented in Tables 3, C.8, and C.9 are visually represented by the networks in Figs. D.14, D.15, and D.16, clearly illustrating the differentiated impact of the Russia-Ukraine conflict on connectedness across different quantile levels and frequency horizons.

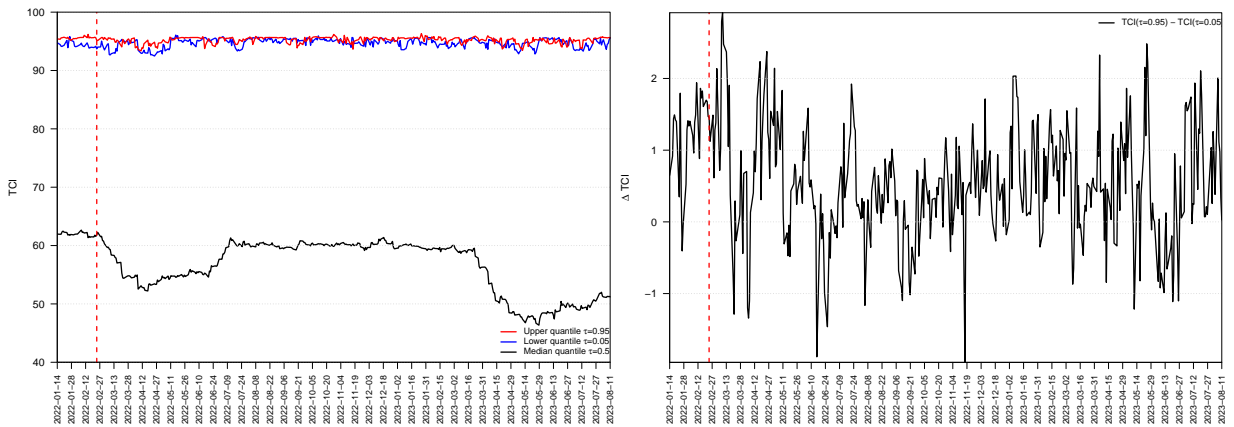


Figure 3: The left plot shows the time-varying total connectedness indices at different quantiles ( $\tau = 0.05, 0.5, 0.95$ ) over time. The right plot shows the relative tail dependence, representing the difference between the TCI at the 95th quantile and the 5th quantile. The vertical dashed line marks the start of the Russia-Ukraine conflict on February 24, 2022.

## 5.2. Dynamic spillover effects of returns in grain futures markets

### 5.2.1. Dynamic total connectedness measures in the time domain

We now examine the time-varying spillover effects among grain futures. By conducting a rolling window analysis on the median, extremely lower, and upper quantiles, we obtain the results presented in Fig. 3. The left panel of Fig. 3 illustrates the TCI at the conditional median quantile, with a general range fluctuating between 46% and 63%, indicating evident temporal heterogeneity. A particularly notable observation is that the dynamic total spillover reaches a high level in the initial phase and remains there, but after the outbreak of the Russia-Ukraine conflict, the TCI drops sharply to its first trough. Following April 20, 2022, it begins a gradual ascent, and by July 15, 2022, the TCI reaches a second peak (just below 60%), and this elevated level persists until March 18, 2023. After March 18, the TCI declines again, reaching its lowest level by the end of May 2023, followed by a slow recovery. Therefore, the first sharp decline in TCI can be primarily attributed to the outbreak of the Russia-Ukraine conflict, which subsequently impacted the grain markets. The second rapid decline in TCI around March 18, 2023, may be due to Russia's decision to shorten the extension period of the Black Sea Grain Initiative to 60 days instead of the usual 120 days<sup>6</sup>, a decision that triggered significant market uncertainty regarding future food supplies, particularly in wheat and corn markets. The first gradual increase in TCI can be attributed to discussions held by the United Nations with Turkey, Russia, and Ukraine on April 25, 26, and 27, 2022, regarding the conflict's impact on the food crisis, which were preliminary discussions for the Black Sea Grain Initiative. The second gradual increase in TCI is partially due to the agreement on May 17 to extend the Black Sea Grain Initiative from May 18 to July 18.

For the dynamic TCI for the left-tail and right-tail distributions, the TCI for both tails fluctuates around 95%, which is significantly higher than the conditional median. This indicates that the TCI is highly sensitive to both downside and upside market conditions. Additionally, shortly after the outbreak of the Russia-Ukraine conflict, we also observe significant fluctuations in the TCI, suggesting that extreme events have a lasting and considerable impact on the TCI. Specifically, the right panel of Fig. 3, which depicts the relative tail dependence of spillovers among grains, reveals that the spillover effects in the left and right tails are asymmetric and heterogeneous. This asymmetry and heterogeneity occur because the spillover effect at the 0.95 quantile is generally stronger than that at the 0.05 quantile and does not exhibit a consistent trend over time. This finding is consistent with Ren et al. (2024), who also reported similar results regarding the spillover effects in the left and right tails.

### 5.2.2. Net total directional connectedness measures in the time domain

Next, Figs. 4, 5, and 6 further illustrate the TO, FROM, and NET total directional connectedness at the median quantile in the time domain, respectively, exploring how the Russia-Ukraine conflict affects the BRICS and international grain markets. Overall, Fig. 4 indicates that BRms, ARs, BRs, USs, ZAwm, ZAym, ARw, ZAc, BSw, ARm, USw, USC, and UAw exhibit relatively strong risk spillovers to other grain futures markets throughout the entire sample period, with Brazilian soybean futures being the most dominant, reaching up to 140% at certain points. In contrast, the TO spillovers from USr, CNc, and INm are moderate (with a maximum not exceeding 40%), while CNr, CNs, and INb exhibit the smallest spillovers to other grain futures markets (with a maximum of less than 20% throughout the sample period). Notably, the impact of the Russia-Ukraine conflict on the TO connectedness from each grain is clearly observable. For instance, the risk spillovers from BRms, BRs, ARs, USs, ARm, BSw, USw, and UAw to other grain markets sharply decreased following the conflict's outbreak, whereas the TO connectedness of grains like ZAw, ARw, and ZAc significantly increased, demonstrating evident heterogeneity.

Correspondingly, Fig. 5 shows that, except for CNr, INb, and INm, which exhibit relatively low FROM connectedness (averaging below 20%), the remaining grains exhibit strong time-varying risk spillovers received from other grain markets, with South African maizes being the strongest (averaging over 80% throughout the sample period). Unlike TO connectedness, in the early stages following the outbreak of the Russia-Ukraine conflict, the FROM connectedness of almost every grain shows a declining trend. In particular, the TO and FROM connectedness of U.S. wheat and Brazilian soybean futures responded the fastest to the conflict.

Moving ahead, we present the dynamic net interlinkages between grain futures markets, representing the combined effect of TO minus FROM. By categorizing the spillover index into two levels, namely across multiple investment

<sup>6</sup>Press Releases and Statements on the Black Sea Grain Initiative can be found at: <https://www.un.org/en/black-sea-grain-initiative/uploads>.

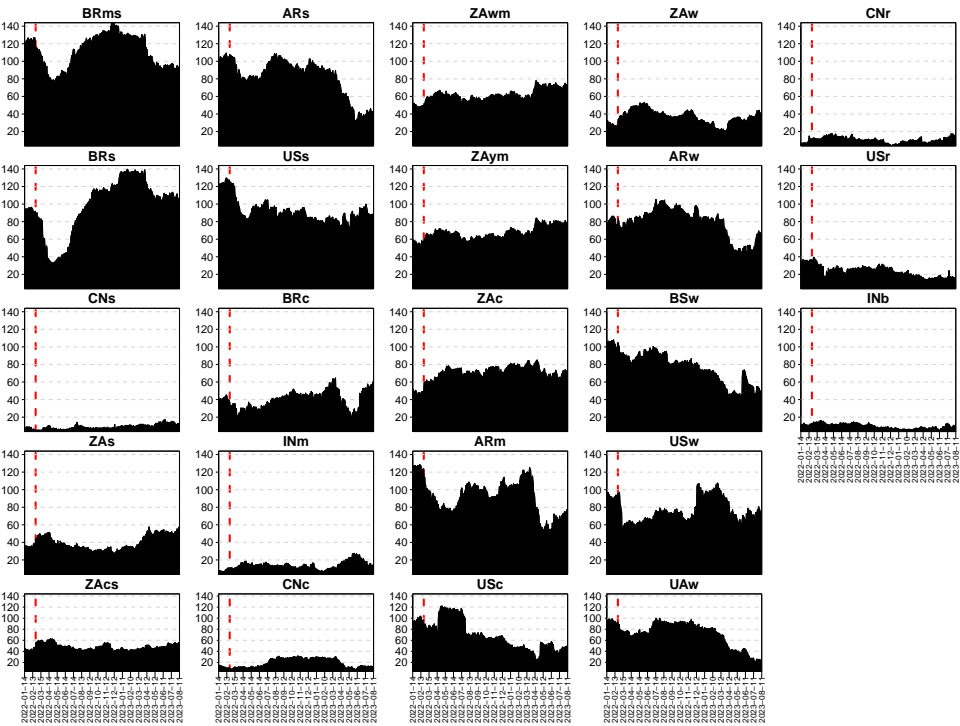


Figure 4: TO connectedness at the 0.5 quantile in the time domain.

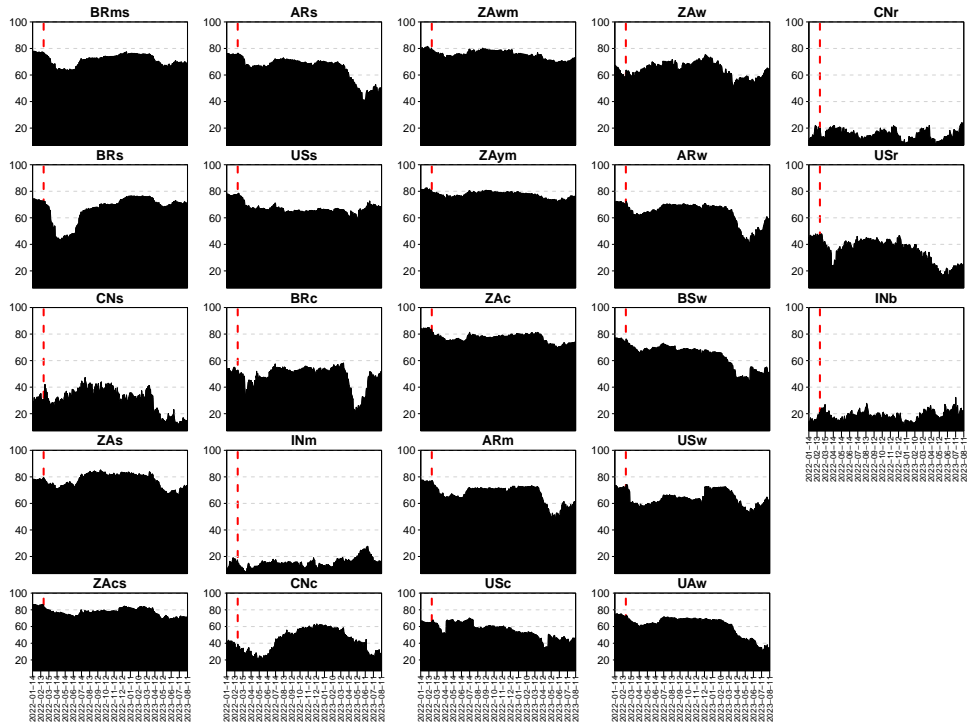


Figure 5: FROM connectedness at the 0.5 quantile in the time domain.

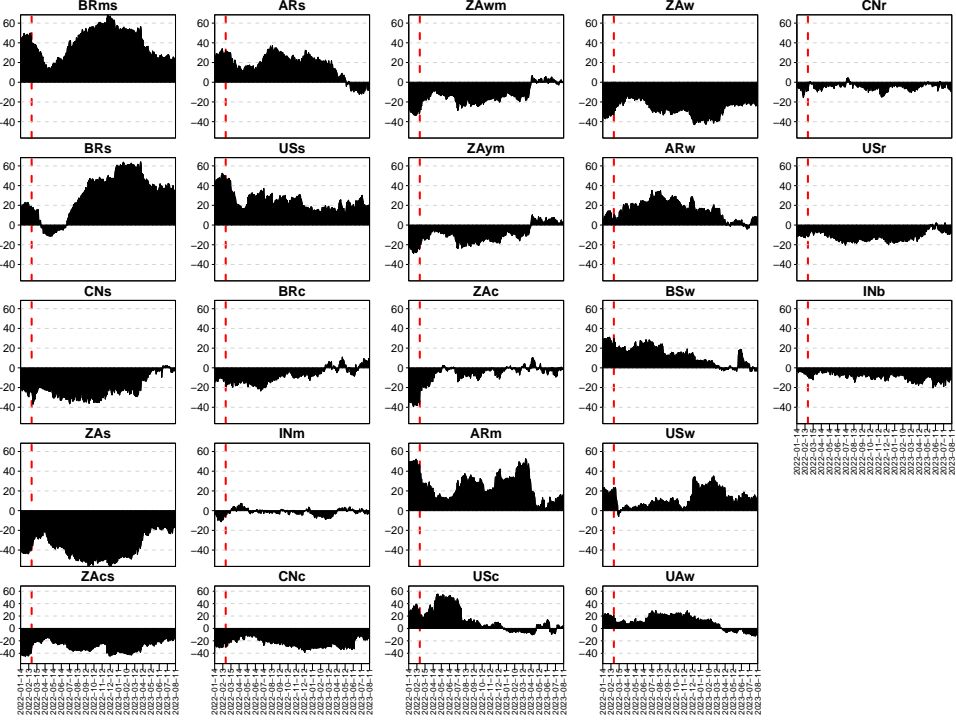


Figure 6: NET connectedness at the 0.5 quantile in the time domain.

horizons and multiple market conditions, we reveal the dynamics of connectedness over short-, medium-, and long-term periods under normal and extreme market conditions, as shown in Figs. 6, 9, B.12, and B.13. We begin by showcasing the time domain spillover results at the 0.5 quantile level in Fig. 6. Of note, for the net total directional connectedness shown in Fig. 6, as explained in Section 4, positive values indicate net contributors of shocks, while negative values indicate net receivers of systemic shocks. BRms, USs, ARw, BSw, ARm, and USw consistently exhibited positive net return connectedness throughout the sample period, serving as net transmitters of systemic shocks. In contrast, ZAw, CNr, USr, CNs, INb, ZAs, ZAcs, and CNc remained net receivers of spillovers over the entire sample period. However, ZAwm and ZAym were net receivers of spillover effects until late March 2023, after which they transitioned to net transmitters. Overall, for most of the sample period, they largely functioned as net receivers. Conversely, UAw exhibited the opposite pattern, acting as a net transmitter in the earlier period but transitioning to a net receiver of shocks after late March 2023. This shift could be related to the shortening of the extension period of the Black Sea Grain Initiative. Thus, for UAw, the net transmitting risk effect predominates. Regarding BRs, it was a net transmitter before April 2022, shifted to a net receiver between April and July, and became a net contributor of shocks after July 2022, with the intensity of risk transmission increasing rapidly, particularly following the successful implementation of the Black Sea Grain Initiative. BRc, ZAc, and INm, on the other hand, tended to be net receivers of spillover effects for most of the earlier part of the sample period. Coincidentally, the impact of the Russia-Ukraine conflict on NET connectedness is evident in Fig. 6, where a structural shift in the evolution of NET connectedness can be observed. Moreover, the Black Sea Grain Initiative also has a significant impact on the dynamic TO, FROM, and NET connectedness, as all three connectednesses show noticeable changes following the renewal of the Black Sea Grain Initiative on March 18, 2023, as depicted in Figs. 4, 5, and 6.

The TO, FROM, and NET connectedness discussed above all pertain to spillover effects under normal market conditions. Next, we will further analyze the time-varying spillover effects under extreme bearish and bullish market environments. Fig. B.12 displays TO, FROM, and NET connectedness at the left ( $\tau = 0.05$ ) and right tails ( $\tau = 0.95$ ) in the time domain. The TO and FROM connectedness at both the left and right tails remain consistently strong, unlike the 0.5 quantile, where some grains exhibit weaker connectedness. Throughout the sample period, TO connectedness

at both tails generally exceeds 100%. In the left tail, some grains reach TO values as high as 500%, indicating a strong spillover effect. In the right tail, certain grains show TO spillover well beyond 500%, with Black Sea wheat futures being the most dominant, surpassing 900% by the end of August 2022—an extremely strong spillover effect. The impact of the Russia-Ukraine conflict is also evident; for instance, the TO connectedness of Ukrainian wheat futures in the right tail dropped sharply from around 780% to approximately 100% following the outbreak of the conflict. The FROM connectedness at both tails hovers around 95%, but on average, the right tail's FROM connectedness is higher than that of the left tail, aligning with our conclusions about static connectedness. Meanwhile, the NET connectedness at the left and right tails alternates between positive and negative values, differing from the 0.5 quantile, where no single grain consistently acts as a net transmitter or receiver throughout the sample period. However, the overall spillover effect for each grain varies, with some grains predominantly acting as net transmitters and others as net receivers most of the time. The asymmetry between the left and right tails is also easily identifiable in the dynamic TO, FROM, and NET connectedness.

### *5.2.3. Net pairwise directional connectedness measures in the time domain*

Fig. 7 shows the dynamic net pairwise directional connectedness of returns, highlighting the net spillovers between two return series and how each grain futures market impacts the others. Likewise, positive values indicate net transmitters of shocks, while negative values indicate net receivers.

First, Brazilian soybean futures consistently acted as a dominant transmitter to the vast majority of grain markets throughout the entire sample period. This is especially true for soybean futures markets in other BRICS countries, which received high levels of spillovers from Brazilian soybeans. The spillover effects initially declined following the outbreak of the Russia-Ukraine conflict, but continued to increase with the announcement of the Black Sea Grain Initiative, reaching a peak before gradually weakening. Specifically, Brazilian soybean futures were constantly dominated by the U.S. soybean futures market before the announcement of the Black Sea Grain Initiative. However, after the initiative, they became a consistent net transmitter of shocks.

In the net pairwise spillovers between China's soybean futures and other grain futures, most grains primarily transmit spillovers to China's soybeans, with USs, BSw, and UAw showing relatively strong spillovers for a period following the outbreak of the conflict. Throughout the entire sample period, South African soybean futures were strongly dominated by Argentine soybean, U.S. soybean, and Argentine wheat futures. Similarly, South African maize futures were dominated by U.S. corn futures, and South African wheat futures were consistently dominated by Argentine wheat, Black Sea wheat, U.S. wheat, and Ukrainian wheat futures.

Before the announcement of the Black Sea Grain Initiative, Black Sea wheat futures transmitted risk to Ukrainian wheat futures. After the initiative, Ukrainian wheat futures became the net transmitter of shocks. Overall, as a benchmark for international grain prices, U.S. grain futures generally held a dominant position in the net pairwise spillover, influencing the grain futures markets of BRICS countries for the majority of the time.



Figure 7: Dynamic net pairwise directional connectedness at the 0.5 quantile in the time domain.

Additionally, under normal market conditions, the net pairwise directional connectedness between similar grain futures markets is relatively strongest, which is also reasonable.

#### 5.2.4. Dynamic total connectedness measures in the frequency domain

Fig. 8 illustrates the time-varying total connectedness at short-, medium-, and long-term frequencies. Under normal market conditions, the overall total connectedness primarily originates from the short-term, with a similar evolutionary pattern. The two sudden declines in short-term connectedness correspond to the outbreak of the Russia-Ukraine conflict and changes in the Black Sea Grain Initiative.

In contrast, the overall total connectedness is slightly influenced by medium- and long-term systemic shocks, with medium-term connectedness ranging from 5% to 10% and long-term connectedness below 5% throughout the sample period.

Under extreme market conditions, a consistent observation is that, similar to the 0.5 quantile, overall total connectedness is predominantly driven by short-term shocks during most periods. However, medium- and long-term connectedness also emerge as significant contributors in specific intervals. Fig. 8 also highlights the asymmetry in total connectedness between the left and right tails, as well as the fact that medium-term connectedness does not consistently remain stronger than long-term connectedness in these tails.

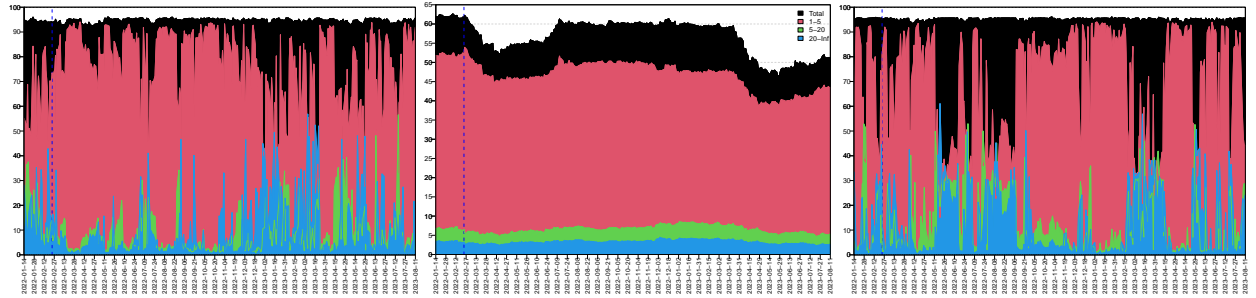


Figure 8: Short-term, medium-term, long-term, and overall dynamic total connectedness in the frequency domain. The left, middle, and right subfigures correspond to the extreme lower ( $\tau = 0.05$ ), conditional median ( $\tau = 0.5$ ), and extreme upper ( $\tau = 0.95$ ) quantiles, respectively.

#### 5.2.5. Net total directional connectedness measures in the frequency domain

Fig. 9 plots the time-varying NET spillover indexes for all grain futures markets at the median quantile in the frequency domain. It reveals that some grains consistently act as transmitters of shocks across short-, medium-, and long-term frequencies, such as BRms and USs, while others are receivers, such as USr and INB. Similar to the characteristics of Fig. 8, the strongest net spillover effect in each grain market comes from the short-term frequency, followed by the medium-term, with the smallest impact from the long-term. This indicates that in the grain futures markets, the gap between transmitted or received shocks from the system is smallest in the long term. Moreover, Fig. 9, whose time-varying trend is influenced by the Russia-Ukraine conflict and the significant policy announcements we discussed previously, reflects a similar evolutionary pattern to Fig. 6.

### 5.3. Sensitivity to quantiles

To further indicate the fluctuations of the total spillover, we visualized the sensitivity of return connectedness to various quantiles (bearish, moderate, and bullish) in both the time domain and the frequency domain using heatmaps. Fig. 10 shows the dynamic total connectedness over time and quantiles in the time domain, where warmer shades on the heatmap represent higher levels of connectedness. Fig. E.17 depicts the short-term, medium-term, and long-term dynamic total connectedness over time and quantiles, respectively.

At first glance at Fig. 10, the total connectedness shows a hot red shade below the 25th quantile and above the 75th quantile, demonstrating strong interlinkages throughout the entire sample period. For all market conditions between the 0.3 and 0.7 quantiles, a significant decline in connectedness among grain futures can be observed following the outbreak of the Russia-Ukraine conflict and the shortening of the Black Sea Grain Initiative. Broadly speaking, Fig. 10 exhibits a symmetric spillover effect over time and across quantiles. Approximately, the short-term heatmap visualized

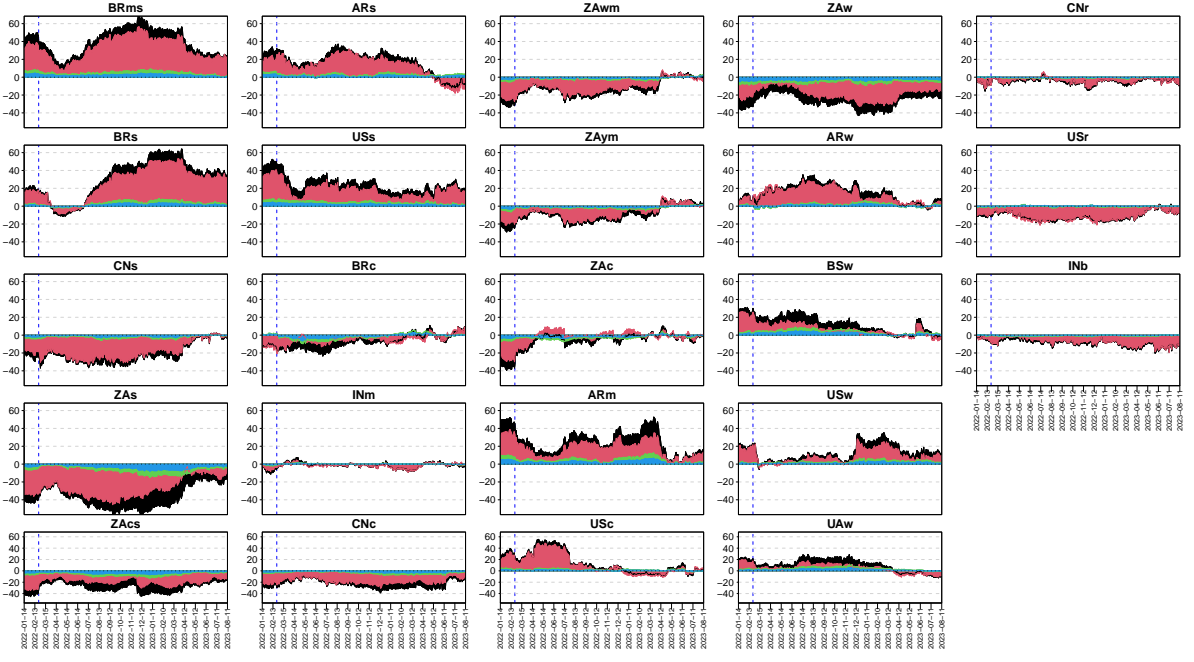


Figure 9: Time-varying NET connectedness at the conditional median ( $\tau = 0.50$ ) quantile in the frequency domain.

in Fig. E.17 closely resembles the overall connectedness heatmap, albeit slightly weaker, while the spillover effect in the medium term is weak across all quantiles and even weaker in the long term. Unlike Fig. 10, Fig. E.17 reveals the asymmetry in connectedness along diverse quantiles. In summary, Fig. E.17 further demonstrates the reliability of total spillover depicted in Fig. 8, showing that, regardless of the quantile, short-term connectedness is always the strongest.

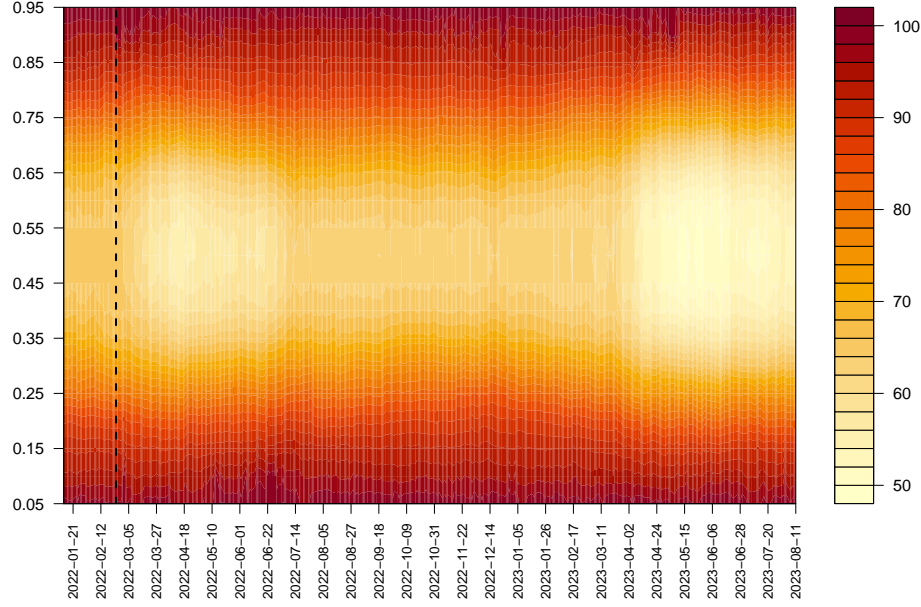


Figure 10: Dynamic total connectedness across time and quantiles in the time domain.

We also carried out an analysis of the sensitivity to quantiles regarding the net total directional connectedness of

each grain futures market. Fig. 11 shows the heatmap of net directional connectedness in the time domain. Figs. E.18 to E.20 are included to illustrate the heatmap of the net total directional connectedness across short-, medium-, and long-term frequencies. In each heatmap, a net-transmitting grain market corresponds to warmer shades (red), while a net-receiving market corresponds to colder shades (blue). The deeper the red or blue areas, the stronger the market's ability to net transmit or receive systemic shocks, and vice versa.

Referring to Fig. 11, the net directional connectedness of each market is heterogeneous and time-varying across quantiles and time periods. However, the graphical representation in Fig. 11 also captures the dominant transmitting features of systemic shocks at various quantile levels in terms of net connectedness, such as BRms, BRs, ARs, USs, ARw, ARm, and USw. Moreover, subsequent to the commencement of the Russia-Ukraine conflict, there is a noticeable change in color shade, signifying a significant shift. Fig. 11 also demonstrates that many grain futures play a mixed role as net receivers and contributors over time and across various quantiles, such as ZAwm, ZAym, ZAc, USc, BSw, and UAw. The shortening of the Black Sea Grain Initiative in March 2023 had different impacts on various grain futures markets; for example, the net spillover heatmap for ZAwm, ZAym, and ZAc shows a deepening red shade after March, while UAw shifts more towards blue. Additionally, USc, BSw, and Uw saw their net transmitter roles gradually weaken following the announcement of the Black Sea Grain Initiative, alternating between the roles of net transmitter and receiver.

Correspondingly, ZAw, ZAs, CNs, INm, CNc, CNr, USr, and INb almost always remained net receivers, except in extreme quantiles (0.95 and 0.05), where the roles of net transmitter and receiver alternated. Notably, we observed significant differences in the net directional connectedness heatmap across quantiles, even for grain futures markets that were net receivers most of the time. For instance, some markets showed weaker net receiving at median quantiles, such as INm and CNr, while others, like ZAs and CNc, exhibited stronger net receiving at median quantiles. Overall, Fig. 11 further illustrates that net directional connectedness is very sensitive to the state of the market, particularly under bullish and bearish conditions.

When considering the quantile sensitivity of the net directional connectedness of each market in the frequency domain, visualized in Figs. E.18 to E.20, what stands out is the striking similarity between the short-term and overall connectedness heatmaps. However, the medium- and long-term connectedness shows notable differences. As an illustration, in the long-term frequency domain, USr does not consistently act as a net receiver across all quantile levels, as depicted in the overall connectedness shown in Fig. 11. Instead, the net transmitting of shocks is its primary role.

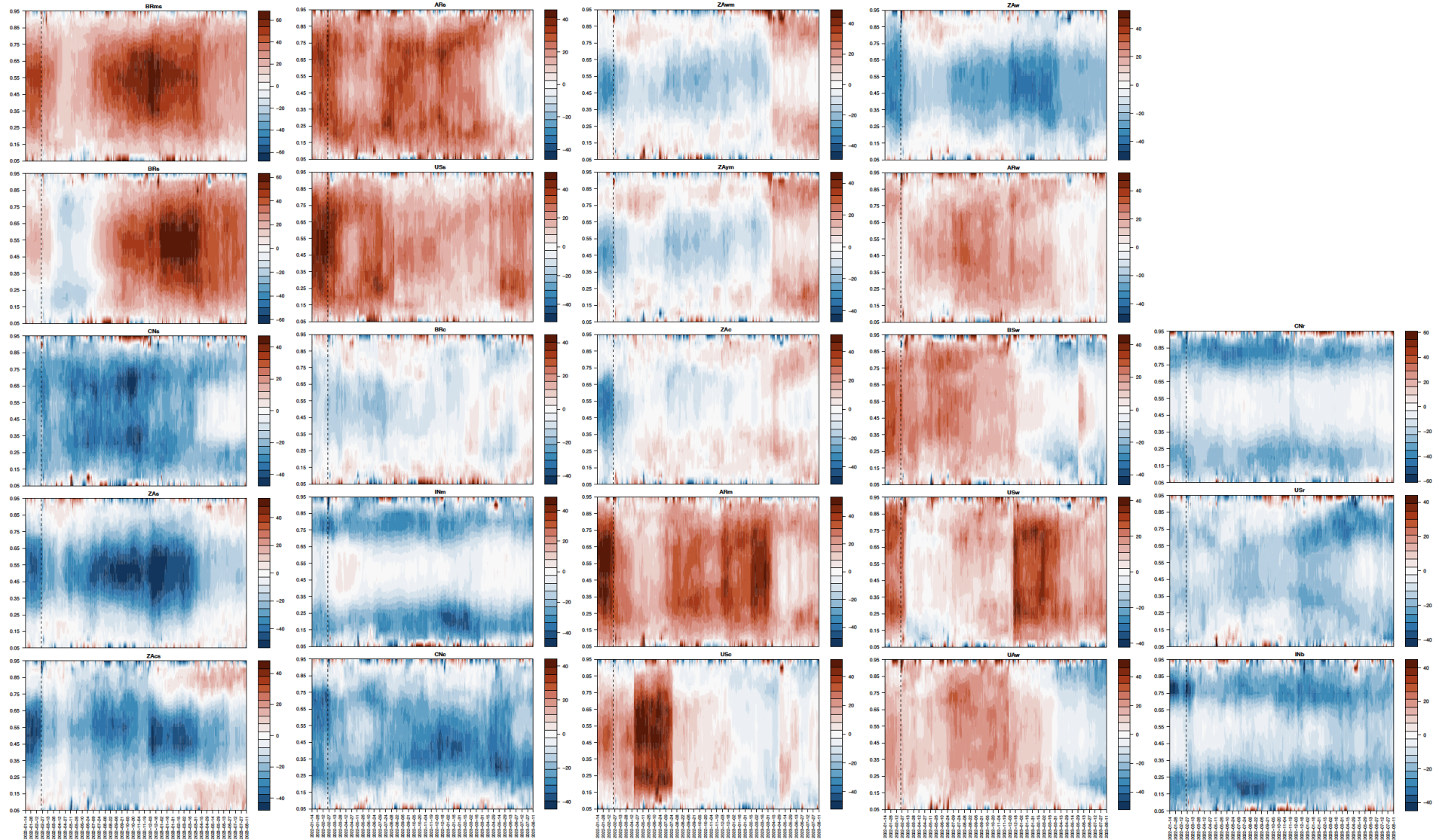


Figure 11: Net total directional connectedness across time and quantiles in the time domain.

## 6. Conclusion

Ensuring global food security is of paramount importance, particularly in times of geopolitical instability, as it directly impacts the well-being of populations, the stability of economies, and the functioning of financial markets (Behnassi and El Haiba, 2022; Zhou et al., 2024a). Grain futures markets, in particular, serve as crucial benchmarks for pricing and risk management, not only within the agricultural sector but also across financial markets. These benchmarks offer essential information that stabilizes markets, informs investment decisions, and ensures a reliable supply of critical commodities, thereby playing a vital role in maintaining both economic and financial stability.

Despite scholars' attention to spillover effects in grain futures markets, most research has focused on spillovers between grain futures and other futures markets (Cui and Maghyereh, 2024; Tiwari et al., 2022; Kumar et al., 2021; Rezitis et al., 2024; Kang et al., 2017; Zhang et al., 2023; Xiao et al., 2020), such as energy futures markets (Rezitis et al., 2024). Only a few studies have concentrated on the internal spillover effects within grain futures markets themselves (Ouyang and Zhang, 2020; Aït-Youcef, 2019; Just and Echaust, 2022; Hamadi et al., 2017; Wang et al., 2024). Moreover, there has been limited exploration of the heterogeneous performance of spillovers among grain futures in major agricultural countries, such as the BRICS nations, under different quantile conditions. Nevertheless, this topic is both compelling and significant, as it can provide valuable insights for investors and policymakers in managing financial risks related to grain commodities.

This study has provided a comprehensive analysis of the quantile connectedness between the BRICS and international grain futures markets, with a particular focus on the impact of the Russia-Ukraine conflict. Specifically, we not only employed the dynamic connectedness approach based on the quantile vector autoregressive model newly developed by Ando et al. (2022), but also utilized the method proposed by Baruník and Křehlík (2018). These methodologies allowed us to provide comprehensive evidence of spillover effects among grain futures from both time and frequency domains, across static and dynamic perspectives, and under both normal and extreme market scenarios.

Our findings demonstrate that the degree of connectedness between these markets is not uniform across different quantiles, indicating that the relationships between these markets vary significantly under normal and extreme market conditions. First, the static connectedness in the time domain indicates that, under both normal and extreme market conditions, each grain futures market largely impacts its own forecast error variance. The TCI was consistently higher during the pre-outbreak period across all quantiles, suggesting weaker interdependence among grain futures markets after the conflict. Particularly, the average dynamic connectedness indicates that both the type of grain and regional proximity play significant roles in strengthening pairwise connectedness among futures markets. Moreover, throughout the entire sample period, South African grain futures tend to be net receivers of shocks, while Argentine grain futures, along with U.S. soybean and Ukrainian wheat futures, typically act as key transmitters of spillovers.

Under extreme bearish market conditions, grain futures such as U.S. corn, wheat, rice, Black Sea wheat, Chinese soybean, and South African maize consistently acted as net receivers of shocks from the pre- to post-outbreak periods, highlighting their persistent vulnerability to external risks. In contrast, Brazilian soybean, Argentine maize, Brazilian corn, Argentine soybean, U.S. soybean, South African wheat, and Ukrainian wheat consistently served as key transmitters of risk. Notably, the Indian grain futures market shifted from being a net receiver to a transmitter, while Argentine wheat futures transitioned into net receivers. Brazilian soybean and corn futures further solidified their roles as dominant risk transmitters post-outbreak, while Ukrainian wheat experienced a significant decline in its transmission capacity.

Under extreme bullish market conditions, notably, Brazilian soybean and corn futures were net recipients pre-outbreak. U.S., Argentine, and Black Sea wheat futures shifted from net receivers to net transmitters post-outbreak, with Black Sea wheat showing the most significant change (from -0.49% to 13.95%), underscoring the impact of the Russia-Ukraine conflict. Meanwhile, South African soybean and Chinese corn reversed their roles from net transmitters to net receivers post-conflict. Ukrainian wheat futures, which were dominant net transmitters pre-outbreak (49.92%), also shifted significantly to become net receivers post-outbreak (-0.67%). At the median quantile, the information transmission mechanism shows distinct differences compared to the lower and upper quantiles across the pre- and post-outbreak periods. South African grain futures consistently served as the main risk absorbers, while Argentine grain futures were the dominant net transmitters of shocks. Noteworthy is the fact that, from the pre- to post-outbreak period, the spillover intensity of most transmitters significantly declined, with Black Sea wheat dropping from 28.32% to 4.24% and Ukrainian wheat from 20.86% to 2.74%, making them the weakest transmitters post-outbreak.

Second, the static results of frequency-domain connectedness unfold that the total spillover within the grain futures system decreases as the frequency increases, with short-term spillovers being dominant. This finding is consistent with conclusions drawn in most other markets ([Liu et al., 2023](#); [Le et al., 2023](#); [Lei et al., 2024](#)). Under extreme market conditions, short-term TCIs increased post-outbreak, while medium- and long-term TCIs were higher pre-outbreak. Conversely, under normal market conditions, the short-, medium-, and long-term TCIs exhibited the opposite pattern.

As for the time-domain perspective of dynamic connectedness, we observed that the dynamic TCI for both the left-tail and right-tail distributions consistently fluctuates around 95%, which is notably higher than the conditional median. Additionally, the systemic risk within the grain futures system is heavily influenced by the onset of the Russia-Ukraine conflict, as well as the signing, modification, and termination of the Black Sea Grain Initiative. Concerning time-varying frequency-based spillovers, overall total connectedness is largely driven by short-term shocks during most periods. Further, dynamic NET spillover analysis indicates that Brazilian soybeans, U.S. soybeans, Argentine wheat, Black Sea wheat, Argentine maize, and U.S. wheat consistently acted as net transmitters of systemic shocks throughout the sample period. In contrast, South African wheat, Chinese rice, U.S. rice, Chinese soybeans, Indian barley, South African soybeans, South African corn, and Chinese corn remained net receivers. Notably, South African white maize and South African yellow maize were net receivers until late March 2023, when they transitioned to net transmitters, while Ukrainian wheat displayed the opposite pattern, shifting from a net transmitter to a net receiver around the same time, possibly due to the shortened extension of the Black Sea Grain Initiative. Overall, U.S. grain futures, serving as a benchmark for international grain prices, consistently held a dominant position in net pairwise spillovers, exerting influence on the grain futures markets of BRICS countries for most of the period. This finding is consistent with [Zhu et al. \(2024\)](#)'s research on risk spillovers between Sino-US agricultural futures.

Finally, the analysis of quantile sensitivity reveals that spillover effects are generally symmetric across quantiles, with a significant decline in connectedness among grain futures observed between the 0.3 and 0.7 quantiles following the Russia-Ukraine conflict and the shortening of the Black Sea Grain Initiative. Notably, while different quantile levels do not significantly change the overall roles of certain grain futures as dominant transmitters or receivers, net directional connectedness remains highly sensitive to market conditions, especially during bullish and bearish periods.

Based on the above findings, our study presents several key implications for both grain futures investors and policymakers. For investors, the results emphasize the importance of strategic portfolio diversification and dynamic risk management. Grain futures that consistently act as net receivers of shocks should be carefully hedged to mitigate vulnerability, while those consistently serving as net transmitters can be leveraged as strategic hedging tools within portfolios. For grain futures that switch roles depending on market conditions, investors should adopt a flexible and adaptive strategy, making frequent portfolio adjustments to optimize returns and manage risks effectively.

For policymakers, the findings highlight the need to enhance market stability and develop robust risk monitoring frameworks. The dominant influence of U.S. grain futures as benchmarks for international grain prices and their significant impact on markets in emerging economies, such as the BRICS countries, underscores the necessity for coordinated international policy efforts to mitigate cascading market shocks. Establishing real-time risk monitoring systems that can adapt to varying degrees of spillover effects observed across different quantiles is crucial. This includes not only regular risk assessments but also the development of strategies to manage the short-term impacts of geopolitical events, such as the Russia-Ukraine conflict, on global food markets. Moreover, to maintain market confidence and stability, policymakers should prioritize transparency in market operations and clearly communicate the implications of major policy changes, such as those related to the Black Sea Grain Initiative. Strengthening international cooperation and creating comprehensive regulatory frameworks will be essential in reducing systemic risks and ensuring the smooth functioning of global grain futures markets.

Several limitations could be addressed in future research. First, the analysis is limited by the data available up to August 11, 2023, for Black Sea and Ukrainian wheat futures. New data may provide further insights into spillover effects among grain futures. Second, while this study focuses on connectedness across different quantiles and frequencies, future research could explore contemporaneous and lagged connectedness for a deeper understanding of spillovers ([Balli et al., 2023](#)). Additionally, expanding the analysis to other emerging markets or different geopolitical events could offer a more comprehensive view of market dynamics.

## References

- Aït-Youcef, C., 2019. How index investment impacts commodities: A story about the financialization of agricultural commodities. *Economic Modelling* 80, 23–33. doi:[10.1016/j.econmod.2018.04.007](https://doi.org/10.1016/j.econmod.2018.04.007).
- Ando, T., Greenwood-Nimmo, M., Shin, Y., 2022. Quantile Connectedness: Modeling Tail Behaviorin the Topology of Financial Networks. *Management Science* 68, 2401–2431. doi:[10.1287/mnsc.2021.3984](https://doi.org/10.1287/mnsc.2021.3984).
- Balli, F., Balli, H.O., Dang, T.H.N., Gabauer, D., 2023. Contemporaneous and lagged R2 decomposed connectedness approach: New evidence from the energy futures market. *Finance Research Letters* 57, 104168. doi:[10.1016/j.frl.2023.104168](https://doi.org/10.1016/j.frl.2023.104168).
- Baruník, J., Křehlík, T., 2018. Measuring the frequency dynamics of financial connectedness and systemic risk. *Journal of Financial Econometrics* 16, 271–296. doi:[10.1093/jjfinec/nby001](https://doi.org/10.1093/jjfinec/nby001).
- Behnassi, M., El Haiba, M., 2022. Implications of the Russia–Ukraine war for global food security. *Nature Human Behaviour* 6, 754–755. doi:[10.1038/s41562-022-01391-x](https://doi.org/10.1038/s41562-022-01391-x).
- Chatziantoniou, I., Gabauer, D., Stenfors, A., 2021. Interest rate swaps and the transmission mechanism of monetary policy: A quantile connectedness approach. *Economics Letters* 204, 109891. doi:[10.1016/j.econlet.2021.109891](https://doi.org/10.1016/j.econlet.2021.109891).
- Chen, Q., Weng, X., 2018. Information flows between the US and China's agricultural commodity futures markets—based on VAR–BEKK–Skew-t model. *Emerging Markets Finance and Trade* 54, 71–87. doi:[10.1080/1540496X.2016.1230492](https://doi.org/10.1080/1540496X.2016.1230492).
- Cui, J., Maghyereh, A., 2024. Unveiling interconnectedness: Exploring higher-order moments among energy, precious metals, industrial metals, and agricultural commodities in the context of geopolitical risks and systemic stress. *Journal of Commodity Markets* 33, 100380. doi:[10.1016/j.jcomm.2023.100380](https://doi.org/10.1016/j.jcomm.2023.100380).
- Diebold, F.X., Yilmaz, K., 2014. On the network topology of variance decompositions: Measuring the connectedness of financial firms. *Journal of Econometrics* 182, 119–134. doi:[10.1016/j.jeconom.2014.04.012](https://doi.org/10.1016/j.jeconom.2014.04.012).
- Ding, Q., Huang, J., Chen, J., 2023. Time-frequency spillovers and the determinants among fossil energy, clean energy and metal markets. *The Energy Journal* 44, 259–286. doi:[10.5547/01956574.44.2.q](https://doi.org/10.5547/01956574.44.2.q).
- Gao, X.L., Shao, Y.H., Yang, Y.H., Zhou, W.X., 2022. Do the global grain spot markets exhibit multifractal nature? *Chaos, Solitons & Fractals* 164, 112663. doi:[10.1016/j.chaos.2022.112663](https://doi.org/10.1016/j.chaos.2022.112663).
- Gong, X.L., Zhao, M., Wu, Z.C., Jia, K.W., Xiong, X., 2023. Research on tail risk contagion in international energy markets—the quantile time-frequency volatility spillover perspective. *Energy Economics* 121, 106678. doi:[10.1016/j.eneco.2023.106678](https://doi.org/10.1016/j.eneco.2023.106678).
- Hamadi, H., Bassil, C., Nehme, T., 2017. News surprises and volatility spillover among agricultural commodities: The case of corn, wheat, soybean and soybean oil. *Research in International Business and Finance* 41, 148–157. doi:[10.1016/j.ribaf.2017.04.006](https://doi.org/10.1016/j.ribaf.2017.04.006).
- Han, L., Liang, R., Tang, K., 2013. Cross-market soybean futures price discovery: does the Dalian Commodity Exchange affect the Chicago Board of Trade? *Quantitative Finance* 13, 613–626. doi:[10.1080/14697688.2013.775477](https://doi.org/10.1080/14697688.2013.775477).
- Hu, X., Zhu, B., Zhang, B., Zeng, L., 2024. Extreme risk spillovers between US and Chinese agricultural futures markets in crises: A dependence-switching copula-CoVaR model. *Plos one* 19, e0299237. doi:[10.1371/journal.pone.0299237](https://doi.org/10.1371/journal.pone.0299237).
- Jiang, H., Su, J.J., Todorova, N., Roca, E., 2016. Spillovers and directional predictability with a cross-quantilogram analysis: The case of US and Chinese agricultural futures. *Journal of Futures Markets* 36, 1231–1255. doi:[10.1002/fut.21779](https://doi.org/10.1002/fut.21779).
- Jiang, H., Todorova, N., Roca, E., Su, J.J., 2017. Dynamics of volatility transmission between the US and the Chinese agricultural futures markets. *Applied economics* 49, 3435–3452. doi:[10.1080/00036846.2016.1262517](https://doi.org/10.1080/00036846.2016.1262517).
- Jiang, W., Chen, Y., 2024. Impact of Russia-Ukraine conflict on the time-frequency and quantile connectedness between energy, metal and agricultural markets. *Resources Policy* 88, 104376. doi:[10.1016/j.resourpol.2023.104376](https://doi.org/10.1016/j.resourpol.2023.104376).
- Just, M., Echaust, K., 2022. Dynamic spillover transmission in agricultural commodity markets: what has changed after the COVID-19 threat? *Economics Letters* 217, 110671. doi:[10.1016/j.econlet.2022.110671](https://doi.org/10.1016/j.econlet.2022.110671).
- Kang, S.H., McIver, R., Yoon, S.M., 2017. Dynamic spillover effects among crude oil, precious metal, and agricultural commodity futures markets. *Energy Economics* 62, 19–32. doi:[10.1016/j.eneco.2016.12.011](https://doi.org/10.1016/j.eneco.2016.12.011).
- Ke, Y., Li, C., McKenzie, A.M., Liu, P., 2019. Risk Transmission between Chinese and US agricultural commodity futures markets—A CoVaR approach. *Sustainability* 11, 239. doi:[10.3390/su11010239](https://doi.org/10.3390/su11010239).
- Kumar, S., Tiwari, A.K., Raheem, I.D., Hille, E., 2021. Time-varying dependence structure between oil and agricultural commodity markets: A dependence-switching CoVaR copula approach. *Resources Policy* 72, 102049. doi:[10.1016/j.resourpol.2021.102049](https://doi.org/10.1016/j.resourpol.2021.102049).
- Le, T.H., Pham, L., Do, H.X., 2023. Price risk transmissions in the water-energy-food nexus: Impacts of climate risks and portfolio implications. *Energy Economics* 124, 106787. doi:[10.1016/j.eneco.2023.106787](https://doi.org/10.1016/j.eneco.2023.106787).
- Lei, H., Xue, M., Ye, J., 2024. The nexus between ReFi, carbon, fossil energy, and clean energy assets: Quantile time–frequency connectedness and portfolio implications. *Energy Economics* 132, 107456. doi:[10.1016/j.eneco.2024.107456](https://doi.org/10.1016/j.eneco.2024.107456).
- Li, C., Hayes, D.J., 2017. Price discovery on the international soybean futures markets: A threshold co-integration approach. *Journal of Futures Markets* 37, 52–70. doi:[10.1002/fut.21794](https://doi.org/10.1002/fut.21794).
- Liu, Y., Lu, J., Shi, F., 2023. Spillover relationship between different oil shocks and high-and low-carbon assets: An analysis based on time-frequency spillover effects. *Finance Research Letters* 58, 104516. doi:[10.1016/j.frl.2023.104516](https://doi.org/10.1016/j.frl.2023.104516).
- Naeem, M.A., Hamouda, F., Karim, S., 2024. Tail risk spillover effects in commodity markets: A comparative study of crisis periods. *Journal of Commodity Markets* 33, 100370. doi:[10.1016/j.jcomm.2023.100370](https://doi.org/10.1016/j.jcomm.2023.100370).
- Neik, T.X., Siddique, K.H., Mayes, S., Edwards, D., Batley, J., Mabhaudhi, T., Song, B.K., Massawe, F., 2023. Diversifying agrifood systems to ensure global food security following the Russia–Ukraine crisis. *Frontiers in Sustainable Food Systems* 7, 1124640. doi:[10.3389/fsufs.2023.1124640](https://doi.org/10.3389/fsufs.2023.1124640).
- Ouyang, R., Zhang, X., 2020. Financialization of agricultural commodities: Evidence from China. *Economic Modelling* 85, 381–389. doi:[10.1016/j.econmod.2019.11.009](https://doi.org/10.1016/j.econmod.2019.11.009).
- Ren, Y.S., Klein, T., Jiang, Y., Ma, C.Q., Yang, X.G., 2024. Dynamic spillovers among global oil shocks, economic policy uncertainty, and inflation expectation uncertainty under extreme shocks. *Journal of International Financial Markets, Institutions and Money* 91, 101951. doi:[10.1016/j.intfin.2024.101951](https://doi.org/10.1016/j.intfin.2024.101951).

- Rezitis, A.N., Andrikopoulos, P., Daglis, T., 2024. Assessing the asymmetric volatility linkages of energy and agricultural commodity futures during low and high volatility regimes. *Journal of Futures Markets* 44, 451–483. doi:[10.1002/fut.22477](https://doi.org/10.1002/fut.22477).
- Shao, Y.H., Yang, Y.H., Shao, H.L., Stanley, H.E., 2019. Time-varying lead-lag structure between the crude oil spot and futures markets. *Physica A: Statistical Mechanics and Its Applications* 523, 723–733. doi:[10.1016/j.physa.2019.03.002](https://doi.org/10.1016/j.physa.2019.03.002).
- Tiwari, A.K., Abakah, E.J.A., Adewuyi, A.O., Lee, C.C., 2022. Quantile risk spillovers between energy and agricultural commodity markets: Evidence from pre and during COVID-19 outbreak. *Energy Economics* 113, 106235. doi:[10.1016/j.eneco.2022.106235](https://doi.org/10.1016/j.eneco.2022.106235).
- Wang, H., Dong, Y., Sun, M., Shi, B., Ji, H., 2024. Dynamic dependence of futures basis between the Chinese and international grains markets. *Economic Modelling* 130, 106584. doi:[10.1016/j.econmod.2023.106584](https://doi.org/10.1016/j.econmod.2023.106584).
- Wei, Y., Wang, Y., Vigne, S.A., Ma, Z., 2023. Alarming contagion effects: the dangerous ripple effect of extreme price spillovers across crude oil, carbon emission allowance, and agriculture futures markets. *Journal of International Financial Markets, Institutions and Money* 88, 101821. doi:[10.1016/j.intfin.2023.101821](https://doi.org/10.1016/j.intfin.2023.101821).
- Wu, Y., Ren, W., Wan, J., Liu, X., 2023. Time-frequency volatility connectedness between fossil energy and agricultural commodities: Comparing the COVID-19 pandemic with the Russia-Ukraine conflict. *Finance Research Letters* 55, 103866. doi:[10.1016/j.frl.2023.103866](https://doi.org/10.1016/j.frl.2023.103866).
- Xiao, B., Yu, H., Fang, L., Ding, S., 2020. Estimating the connectedness of commodity futures using a network approach. *Journal of Futures Markets* 40, 598–616. doi:[10.1002/fut.22086](https://doi.org/10.1002/fut.22086).
- Yang, Y.H., Shao, Y.H., 2020. Time-dependent lead-lag relationships between the VIX and VIX futures markets. *The North American Journal of Economics and Finance* 53, 101196. doi:[10.1016/j.najef.2020.101196](https://doi.org/10.1016/j.najef.2020.101196).
- Yang, Y.H., Shao, Y.H., Zhou, W.X., 2024. Contemporaneous and lagged spillovers across crude oil, carbon emission allowance, climate change, and agriculture futures markets: Evidence from the  $R^2$  decomposed connectedness approach. *arXiv preprint arXiv:2408.09669*.
- Zhang, X., Yang, X., Li, J., Hao, J., 2023. Contemporaneous and noncontemporaneous idiosyncratic risk spillovers in commodity futures markets: A novel network topology approach. *Journal of Futures Markets* 43, 705–733. doi:[10.1002/fut.22407](https://doi.org/10.1002/fut.22407).
- Zhang, Y., Sun, Y., Shi, H., Ding, S., Zhao, Y., 2024. COVID-19, the Russia–Ukraine war and the connectedness between the US and Chinese agricultural futures markets. *Humanities and Social Sciences Communications* 11, 1–15. doi:[10.1057/s41599-024-02852-6](https://doi.org/10.1057/s41599-024-02852-6).
- Zhou, W.X., Dai, Y.S., Duong, K.T., Dai, P.F., 2024a. The impact of the Russia-Ukraine conflict on the extreme risk spillovers between agricultural futures and spots. *Journal of Economic Behavior & Organization* 217, 91–111. doi:[10.1016/j.jebo.2023.11.004](https://doi.org/10.1016/j.jebo.2023.11.004).
- Zhou, X., Enilov, M., Parhi, M., 2024b. Does oil spin the commodity wheel? Quantile connectedness with a common factor error structure across energy and agricultural markets. *Energy Economics* 132, 107468. doi:[10.1016/j.eneco.2024.107468](https://doi.org/10.1016/j.eneco.2024.107468).
- Zhu, H.Y., Dai, P.F., Zhou, W.X., 2024. Uncovering the Sino-US dynamic risk spillovers effects: Evidence from agricultural futures markets. *Journal of Futures Markets* doi:[10.1002/fut.22551](https://doi.org/10.1002/fut.22551).
- Živkov, D., Kuzman, B., Subić, J., 2020. What Bayesian quantiles can tell about volatility transmission between the major agricultural futures? *Agricultural Economics* 66, 215–225. doi:[10.17221/127-2019-AGRICECON](https://doi.org/10.17221/127-2019-AGRICECON).

## Appendix A. Summary statistics for the pre-outbreak and post-outbreak periods

Table A.4: Summary statistics for the pre-outbreak sample period.

	BRms	BRs	CNs	ZAs	ZAcS	ARs	UsS	BRc	InM	CNc	ZAwm	ZAym	ZAc	ARm	USc	ZAw	ARw	BSw	UsW	U Aw	CNr	UsR	InB		
Mean	0.001	0.000	0.000	0.001	0.002	0.002	0.001	0.000	0.001	0.000	0.001	0.001	0.002	0.002	0.001	0.002	0.002	0.000	0.002*	0.000	0.001	0.001			
S.D.	0.014	0.013	0.011	0.013	0.018	0.014	0.016	0.014	0.020	0.008	0.017	0.014	0.021	0.017	0.024	0.007	0.016	0.015	0.019	0.015	0.005	0.013	0.012		
Skew	-1.027***	-1.741***	2.274*	-0.010	-0.553***	-0.759***	0.085	0.036	-0.265*	-0.026	0.013	0.497***	-0.197	-0.612***	-0.146	0.074	0.088	0.473***	0.108	3.635***	-0.024	-0.023			
Ex.Kurt	6.458***	10.792***	2.229***	-0.157	0.667*	4.290***	4.860***	2.143***	1.808***	0.927***	-0.050	-0.103	2.624***	1.233***	21.683***	1.668***	0.898***	0.217	0.296	0.724***	28.580**	8.204***	2.954***		
JB	434.337***	180.246***	49.813***	0.236	4.445***	186.044***	245.188***	43.731***	30.945***	10.793***	0.049	0.049	7.804***	15.843***	4704.930***	27.118***	7.831***	2.810	9.278***	5.396***	8225.718***	63038***	63.693***		
ADF	-256.643***	-232.037***	-196.035***	-202.888***	-185.511***	-240.152***	-232.871***	-265.715***	-214.220***	-265.055***	-231.295***	-229.039***	-239.551***	-167.633***	-256.944***	-247.905***	-202.936***	-240.005***	-184.555***	-299.145***	-198.234***				
PP	199	12.254***	6.231	8.251	13.842	20.373***	240.159***	15.328***	10.758***	13.481	14.793	14.793	15.284***	17.204*	11.400***	13.335***	13.904	13.305	23.243***	17.271*	10.161				
Q(20)	Q'(20)	17.334*	22.140***	13.089	15.909*	14.144	40.524***	34.297***	89.913***	23.670***	7.661	18.196***	39.479***	32.944***	67.953***	3.260	90.206***	25.057***	42.424***	8.996	20.144***	0.743	17.186*		
Kendall's $\rho$	BRms	BRs	CNs	ZAs	ZAcS	ARs	UsS	BRc	InM	CNc	ZAwm	ZAym	ZAc	ARm	USc	ZAw	ARw	BSw	UsW	U Aw	CNr	UsR	InB		
BRms	0.000***	0.605***	0.050	0.190***	0.177***	0.557***	0.685***	0.127***	-0.093***	0.035	0.149***	0.156***	0.151***	0.374***	0.377***	0.081	0.265***	0.260***	0.303***	0.260***	0.023	0.139***	-0.073		
BRs	0.005***	1.000***	0.085	0.161***	0.162***	0.494***	0.543***	0.155***	-0.054	0.047	0.145***	0.156***	0.150***	0.355***	0.343***	0.051	0.238***	0.247***	0.281***	0.230***	0.039	0.123***	-0.068		
CNs	0.050	0.085	1.000***	0.079	0.041	0.064	0.038	-0.029	0.031	0.146***	0.060	0.043	0.024	-0.021	-0.043	0.002	0.050	0.014	0.005	0.055	0.020	0.000			
ZAs	0.190***	0.161***	0.079	1.000***	0.959***	0.145***	0.153***	0.050	-0.021	-0.002	0.093***	0.501***	0.484***	0.116***	0.088***	0.303***	0.102***	0.112***	0.086	0.073	-0.010	0.087	0.006		
ZAcS	0.177***	0.162***	0.041	0.595***	1.000***	0.126***	0.147***	0.089***	-0.041	0.005	0.501***	0.534***	0.557***	0.130***	0.106***	0.060	0.059	0.071	0.029	0.008	0.135***	-0.016			
ARs	0.577***	0.494***	0.064	0.145***	0.126***	1.000***	0.253***	0.127***	-0.086	0.070	0.087	0.090***	0.073	0.346***	0.292***	0.080	0.236***	0.245***	0.274***	0.223***	0.013	0.129***	-0.095***		
UsS	0.685***	0.543***	0.058	0.153***	0.147***	0.553***	1.000***	0.151***	-0.072	0.033	0.132***	0.134***	0.109***	0.378***	0.396***	0.110***	0.253***	0.227***	0.308***	0.203***	0.040	0.176***	-0.058		
BRc	0.158***	0.158***	0.050	0.050	0.050	0.127***	0.127***	0.127***	-0.025	0.025	0.024	0.024	0.024	0.179***	0.179***	0.025	0.064	0.064	0.033***	0.088***	0.065	0.065	-0.055		
InM	0.093***	0.054	0.031	0.041	0.041	0.072	0.010	1.000***	-0.056	-0.050	-0.070	-0.070	-0.017	0.029	-0.012	0.031	0.067	0.021	0.058	0.042	-0.059	0.001	-0.015		
CNs	0.035	0.047	0.146***	-0.002	0.005	0.070	0.038	0.022	-0.076	1.000***	0.066	0.071	0.070	0.029	-0.012	0.031	0.067	0.021	0.058	0.042	-0.059	0.009	-0.016		
ZAwm	0.149***	0.145***	0.060	0.493***	0.501***	0.127***	0.132***	0.080	-0.050	0.066	1.000***	0.860***	0.644***	0.125***	0.109***	0.080***	0.121***	0.084	0.026	0.045	0.028	0.005			
ZAym	0.156***	0.156***	0.043	0.301***	0.34***	0.090***	0.134***	0.084	-0.070	0.071	0.860***	1.000***	0.697***	0.169***	0.137***	0.311***	0.093***	0.120***	0.114***	0.093***	0.015	0.055	-0.010		
ZAc	0.151***	0.150***	0.024	0.484***	0.577***	0.073	0.109***	0.070	-0.070	0.070	0.644***	0.679***	1.000***	0.165***	0.137***	0.305***	0.130***	0.141***	0.129***	0.094***	0.053	0.036	-0.020		
ARm	0.374***	0.355***	-0.021	0.116***	0.130***	0.346***	0.378***	0.180***	-0.067	0.029	0.156***	0.169***	0.165***	1.000***	0.448***	0.069	0.337***	0.355***	0.380***	0.317***	0.016	0.154***	-0.082		
UsC	0.377***	0.343***	-0.043	0.088***	0.106***	0.292***	0.396***	0.202***	-0.017	-0.012	0.125***	0.137***	0.148***	0.448***	1.000***	0.114***	0.323***	0.424***	0.281***	-0.001	0.121***	-0.093***			
ZAw	0.081	0.051	0.002	0.300***	0.321***	0.084	0.108***	0.037	-0.036	0.031	0.301***	0.311***	0.395***	0.069	0.114***	0.139***	0.145***	0.123***	-0.008	0.029	0.036				
ARw	0.265***	0.238***	0.050	0.102***	0.060	0.236***	0.248***	0.253***	-0.066	0.008	0.089***	0.093***	0.093***	0.337***	0.137***	0.177***	0.087	0.487***	0.441***	0.440***	0.014	0.075	0.016		
BSw	0.260***	0.240***	0.040	0.112***	0.050	0.242***	0.242***	0.242***	-0.025	0.025	0.024	0.024	0.024	0.481***	0.137***	0.198***	0.088***	0.481***	1.000***	-0.008	0.028	0.032			
U Aw	0.260***	0.230***	0.036	0.073	0.029	0.223***	0.203***	0.082	-0.022	0.068	0.084	0.039***	0.040***	0.040***	0.261***	0.107***	0.281***	0.123***	0.440***	0.778***	0.466***	1.000***	-0.040	0.018	0.080
CNr	0.023	0.039	0.055	-0.010	0.008	0.013	0.040	0.051	0.039	0.042	0.026	0.015	0.053	0.006	-0.001	0.004	-0.004	0.010	-0.021	-0.040	1.000***	0.068	-0.008		
UsR	0.139***	0.123***	0.020	0.087	0.035	0.129***	0.176***	0.068	0.003	-0.059	0.045	0.055	0.036	0.014	0.121***	0.029	0.075	0.028	0.123***	0.018	0.068	1.000***	-0.046		
InB	-0.073	-0.088	0.000	0.006	-0.016	-0.059***	-0.058	-0.055	-0.015	-0.018	-0.028	-0.010	-0.020	-0.082	-0.093***	0.016	0.016	0.032	-0.040	0.080	-0.008	-0.046	1.000***		

Notes: JB represents the Jarque-Bera normality test statistic; ADF represents the Augmented Dickey-Fuller test statistic; PP represents the Phillips-Perron test statistic; Q(n) and  $Q^2(n)$  represent the Ljung-Box Q statistic for testing autocorrelation and autocorrelation in the squared residuals up to lag  $n$ , respectively; \* indicates 10% significance level, \*\* indicates 5% significance level, \*\*\* indicates 1% significance level.

Table A.5: Summary statistics for the post-outbreak sample period.

	BRms	BRs	CNs	ZAs	ZAcS	ARs	UsS	BRc	InM	CNc	ZAwm	ZAym	ZAc	ARm	USc	ZAw	ARw	BSw	UsW	U Aw	CNr	UsR	InB	
Mean	0.000	0.000	-0.001	0.000	0.001	-0.001	-0.001	0.000	0.000	0.000	0.000	0.000	-0.001	0.000	0.000	-0.001	-0.001	-0.001	0.000	0.000	0.000	0.000		
S.D.	0.014	0.014	0.010	0.013	0.015	0.012	0.017	0.013	0.014	0.008	0.015	0.013	0.019	0.015	0.019	0.015	0.020	0.010	0.013	0.004	0.016	0.015		
Skew	-0.009***	-0.009***	0.000	0.000	0.000	0.000	0.000	0.000	0.000	0.000	0.000	0.000	0.000	0.000	0.000	0.000	0.000	0.000	0.000	0.000	0.000	0.000		
Ex.Kurt	6.382***	2.813***	0.089***	0.202	0.166***	0.157***	0.148***	0.127***	0.127***	0.127***	0.127***	0.127***	0.127***	0.127***	0.127***	0.127***	0.127***	0.127***	0.127***	0.127***	0.127***	0.127***		
JB	9.318***	126.649***	25.669***	0.652	89.1796***	41.332***	133.928***	77.011***	26.807***	93.725***	4.040	4.959***	184.518***	134.339***	409.573***	267.769***	23.261***	308.573***	296.777***	164.620***	876.061***	592.231***	5280.547***	97.015***
ADF	-5.730***	-6.134***	-4.695***	-5.679***	-6.543***	-7.176***	-5.888***	-5.636***	-6.597***	-6.007***	-6.309***	-6.427***	-6.508***	-6.786***	-6.670***	-6.648***	-6.355***	-4.424***	-8.445***	-5.030***	-7.348***	-4.746***		
PP	-305.470***	-285.662***	-287.379***	-312.233***	-378.552***	-378.216***	-440.994***	-392.335***	-351.343***	-391.279***	-305.920***	-338.884***	-400.060***	-385.174***	-386.405***	-374.413***	-277.215***	-417.439***	-417.439***	-417.439***	-417.439***	-417.439***		
Q(20)	Q'(20)	21.004***	29.223***	14.182	24.796***	20.965***	23.831***	22.454***	16.379***	15.197	6.658	5.465	7.550	10.905	29.788***	28.282***	18.134***	19.452***	10.449	27.285***	35.561***	20.		

## Appendix B. TO, FROM, and NET connectedness at the left and right tails

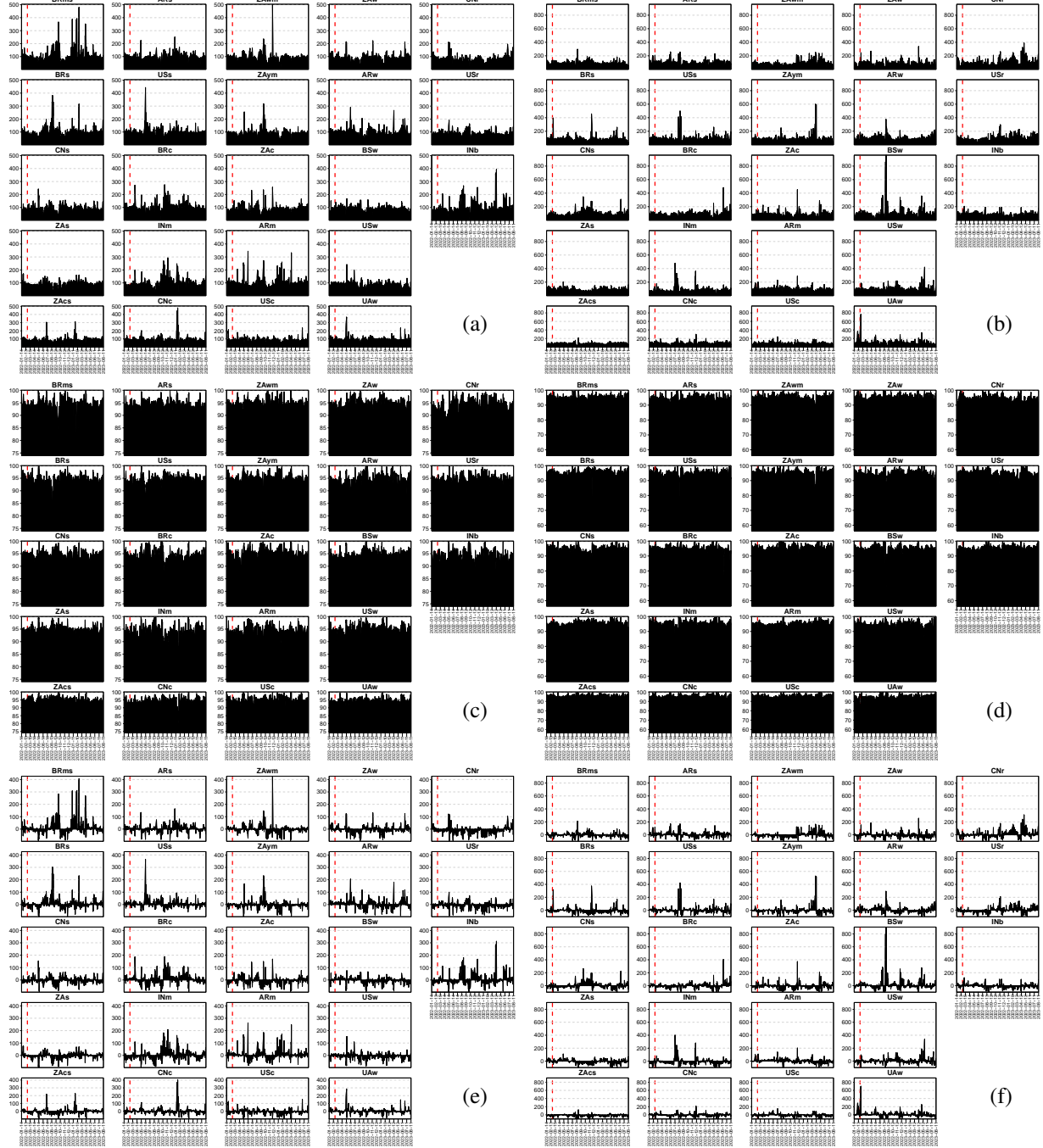


Figure B.12: (a) and (b) show TO connectedness, (c) and (d) display FROM connectedness, and (e) and (f) represent NET connectedness at the left ( $\tau = 0.05$ ) and right tails ( $\tau = 0.95$ ) in the time domain, respectively.

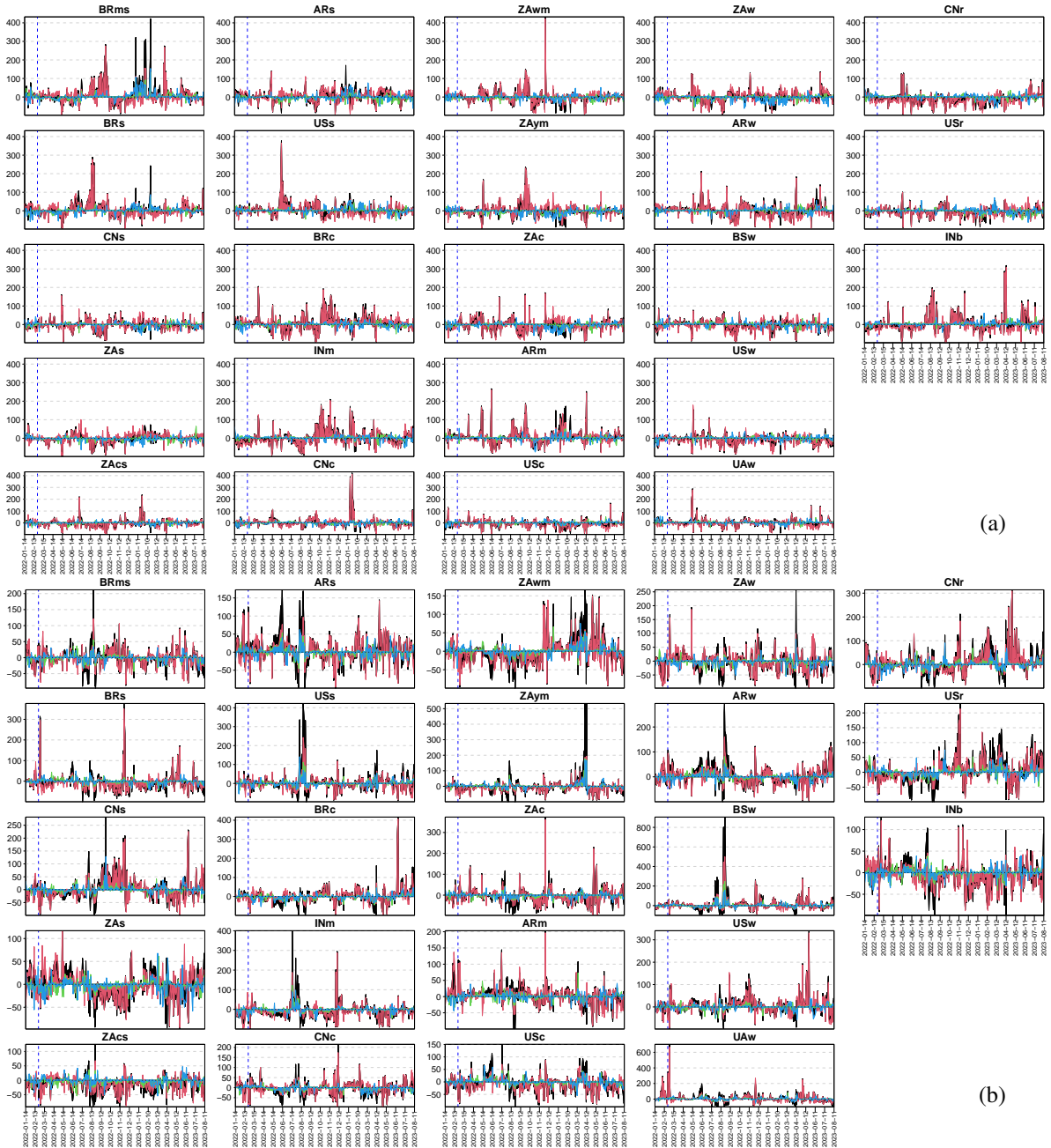


Figure B.13: (a) and (b) show time-varying NET connectedness at the left ( $\tau = 0.05$ ) and right tails ( $\tau = 0.95$ ) in the frequency domain, respectively.

## Appendix C. Average connectedness for the pre-outbreak and post-outbreak periods

Table C.6: Average dynamic connectedness in the time domain at different quantile levels over the pre-outbreak period.

	BRms	BRs	CNs	ZAs	ZAcS	ARs	UsS	BRc	INm	CNc	ZAwM	ZAym	ZAc	ARm	Usc	ZAw	ARw	Bsw	UsW	Uaw	CNr	Usr	INb	FROM
<i>Panel A: Lower quantile (<math>\tau=0.05</math>)</i>																								
BRms	5.46	4.50	4.01	4.73	4.39	4.63	5.03	4.19	3.42	4.59	4.50	4.04	3.43	5.24	4.17	4.39	4.85	3.74	3.77	4.58	4.73	4.20	3.43	94.54
BRs	5.40	4.96	3.71	4.96	4.79	4.71	4.65	5.06	3.30	4.23	4.40	4.06	3.38	4.62	3.94	5.00	5.21	3.43	3.64	4.89	4.61	4.04	3.01	95.04
CNs	4.48	4.73	4.84	4.09	4.37	4.58	4.83	4.84	3.86	4.47	4.28	3.97	3.74	4.64	4.11	4.04	4.71	4.72	4.09	4.64	4.48	3.59	3.87	95.16
ZAs	4.91	4.55	3.82	5.46	4.93	4.66	5.02	4.64	3.53	3.73	4.58	4.30	3.95	4.89	3.65	4.61	4.64	4.22	3.96	4.23	4.30	3.81	3.61	94.54
ZAcS	5.14	4.39	3.84	4.89	5.48	4.93	5.10	4.74	3.76	3.33	4.84	4.63	4.34	4.89	3.38	4.73	4.79	3.44	3.87	4.20	4.27	3.61	3.39	94.52
ARs	5.85	5.05	3.73	4.59	4.57	5.95	5.10	4.73	3.31	3.78	4.35	4.00	3.38	4.87	3.60	4.70	5.13	3.59	3.81	4.71	4.19	4.05	2.96	94.05
UsS	5.37	4.83	3.83	4.40	4.23	5.36	5.97	4.40	3.29	3.78	4.35	3.93	3.41	5.15	4.07	4.28	4.85	4.05	3.96	4.69	4.31	4.20	3.28	94.03
BRc	5.74	4.96	3.73	4.65	4.66	5.01	4.51	5.74	3.51	3.96	4.50	4.11	3.57	4.42	3.92	4.84	5.04	3.42	3.54	4.80	4.60	3.70	3.05	94.26
INm	4.38	4.45	4.05	4.32	4.38	4.36	4.77	4.78	5.83	4.03	4.49	4.23	3.85	4.89	3.74	4.29	4.77	3.95	4.07	4.35	4.58	3.51	3.90	94.17
CNc	4.04	4.37	4.30	4.88	4.39	4.44	4.13	4.60	3.27	6.41	4.60	4.17	3.48	4.63	4.43	4.77	4.20	3.69	4.83	4.66	3.61	3.73	93.59	
ZAwM	5.10	4.16	3.58	5.19	4.95	4.53	4.59	4.75	3.33	3.75	5.29	4.92	3.95	4.55	4.29	4.84	4.80	3.77	3.86	4.81	4.21	3.52	3.25	94.71
ZAym	4.90	4.26	3.66	5.12	4.85	4.31	4.45	4.58	3.12	3.99	5.26	4.81	3.88	4.67	5.02	4.72	4.53	4.11	3.87	4.72	4.30	3.49	3.39	95.19
ZAc	4.43	4.60	3.55	5.01	4.94	4.45	4.59	4.76	3.26	3.84	4.77	4.35	4.46	4.66	5.09	4.70	4.58	4.64	3.66	4.89	4.28	3.40	3.07	95.54
ARm	4.81	4.51	3.88	4.55	4.40	4.61	4.92	4.50	3.40	4.45	4.47	4.15	3.59	5.73	3.73	4.36	5.03	4.15	4.17	4.50	4.26	4.08	3.75	94.27
Usc	4.56	4.35	3.64	5.01	4.64	4.72	4.61	4.66	3.39	4.46	4.60	3.90	3.15	4.75	5.82	4.88	4.84	3.97	4.74	4.31	3.75	3.38	94.18	
ZAw	4.85	4.32	3.73	5.14	5.04	4.67	4.34	4.87	3.30	3.92	4.72	4.26	3.54	4.39	3.62	5.70	5.19	3.73	4.15	4.99	4.12	3.85	3.54	94.30
ARw	4.44	4.50	3.79	4.69	4.68	5.26	4.64	5.13	3.38	3.75	4.73	4.32	3.63	4.70	3.52	4.87	5.86	4.00	4.18	4.76	4.05	3.83	3.28	94.14
Bsw	4.34	4.64	4.04	4.32	3.86	4.37	4.28	4.32	3.05	4.43	4.36	3.75	3.36	4.74	4.50	4.08	5.23	6.19	4.78	5.85	4.13	3.87	3.50	93.81
Usw	4.94	4.61	3.90	4.37	4.12	4.77	4.63	4.83	3.54	4.16	4.54	4.16	3.60	4.82	3.53	4.44	5.22	4.50	4.90	4.98	4.08	3.87	3.50	95.10
Uaw	4.03	4.11	3.95	4.81	4.25	4.09	4.14	4.25	3.19	4.97	4.58	3.79	3.12	4.67	5.19	4.50	4.98	5.04	4.27	5.93	4.58	3.90	3.65	94.07
CNr	4.26	4.22	3.93	4.64	4.40	4.29	4.53	4.39	3.73	4.89	4.41	3.89	3.30	4.67	4.40	4.24	4.65	4.18	3.66	4.85	7.25	3.87	3.36	92.75
Usr	4.63	4.38	3.86	4.87	4.57	4.48	4.76	4.44	3.35	4.20	4.47	4.19	3.55	4.80	3.84	4.83	4.99	3.78	3.98	4.58	4.55	5.20	3.70	94.80
Inb	4.63	4.36	4.45	4.50	4.51	4.08	4.41	4.47	3.97	4.83	4.46	4.08	3.80	4.51	4.22	4.35	4.50	3.93	3.89	4.25	4.64	3.69	5.93	94.07
TO	105.24	98.86	84.96	103.72	99.95	101.30	102.03	101.94	75.28	91.53	100.27	91.21	78.99	103.91	89.23	100.61	107.30	88.57	86.76	103.84	96.25	83.44	75.61	2170.82
Inc.Own	110.70	103.83	89.80	109.18	105.44	107.25	108.00	107.68	81.11	97.94	105.56	96.01	83.46	109.64	95.05	106.31	113.17	94.77	91.66	109.78	103.50	88.64	81.54	TCI
NET	10.70	3.83	-10.20	9.18	5.44	7.25	8.00	7.68	-18.89	-2.06	5.56	-3.99	-16.54	9.64	-4.95	6.31	13.17	-5.23	-8.34	9.78	3.50	-11.36	-18.46	94.38
NPT	17.00	12.00	3.00	17.00	16.00	17.00	16.00	16.00	1.00	11.00	12.00	7.00	4.00	19.00	9.00	14.00	19.00	6.00	7.00	16.00	10.00	2.00	2.00	
<i>Panel B: Median quantile (<math>\tau=0.50</math>)</i>																								
BRms	22.75	10.63	0.12	0.52	0.81	11.29	14.94	2.52	0.16	0.12	0.80	0.84	0.58	8.60	0.70	0.70	3.66	4.37	3.97	4.14	0.10	2.76	0.57	77.22
BRs	12.44	26.74	0.06	0.18	0.55	11.54	11.58	4.31	0.54	0.28	0.88	1.14	1.08	8.05	4.13	0.08	2.68	4.33	2.69	3.38	0.04	2.89	0.41	73.26
CNs	1.51	2.68	69.24	0.69	0.53	2.42	2.49	0.91	1.43	3.02	0.45	0.44	0.34	2.37	0.43	1.32	1.05	1.13	1.20	1.09	1.04	3.28	0.92	30.76
ZAs	7.40	2.85	0.20	12.29	11.84	6.21	7.85	1.35	0.13	0.19	5.58	6.01	5.00	5.53	3.09	4.60	1.36	1.72	2.96	1.43	1.31	2.71	0.77	77.81
ZAcS	11.08	3.42	0.17	6.97	14.40	7.24	11.37	2.71	0.12	0.47	3.16	4.07	3.77	5.09	4.32	1.46	1.87	4.06	2.03	0.10	3.41	0.74	85.60	
ARs	12.16	10.58	0.20	0.74	0.80	24.46	14.47	1.98	0.31	0.43	0.95	1.09	0.52	9.75	3.14	0.43	3.58	4.61	3.48	3.66	0.05	1.98	0.64	75.54
UsS	15.02	9.91	0.03	0.47	0.89	13.50	22.82	2.29	0.13	0.19	1.01	0.96	0.49	8.65	5.55	0.62	3.39	3.67	3.87	3.18	0.08	2.85	0.43	77.18
BRc	5.32	7.63	0.38	1.61	1.29	3.94	4.32	47.33	0.43	0.85	1.77	2.23	2.31	5.39	5.20	0.60	1.05	2.11	1.67	1.82	0.44	0.97	1.31	52.67
INm	0.71	2.22	0.55	0.05	0.27	1.20	0.64	0.28	84.83	1.48	0.40	1.14	0.36	1.19	0.11	0.17	0.63	1.05	0.62	1.86	0.10	0.07	0.09	15.17
CNc	1.88	1.69	2.65	0.42	0.29	1.84	0.70	0.79	1.64	60.72	0.18	0.22	0.34	4.22	4.74	0.61	4.76	4.74	1.81	3.90	0.39	0.13	39.28	
ZAwM	3.66	2.86	0.05	5.18	4.61	2.47	4.03	2.28	0.12	0.19	20.01	17.36	10.45	5.51	8.53	2.50	2.12	2.38	2.65	1.84	0.09	0.69	0.42	79.99
ZAym	3.83	2.34	0.09	5.21	5.45	2.25	3.87	2.32	0.31	0.27	16.15	18.68	11.21	5.15	9.75	3.09	1.62	2.65	2.16	2.72	0.09	0.41	0.37	81.32
ZAc	4.35	3.33	0.14	3.70	4.77	2.38	4.58	3.50	0.14	0.18	8.31	9.64	16.00	6.71	14.40	2.72	2.72	3.99	3.49	2.98	0.18	0.59	0.34	84.00
ARm	8.67	7.01	0.28	0.21	0.50	9.56	8.77	3.00	0.38	0.42	0.73	1.00	0.74	23.27	6.37	0.62	6.53	6.72	6.36	5.78	0.08	2.10	0.37	76.73
Usc	7.68	5.50	0.14	0.20	0.45	4.38	4.84	3.52	0.16	0.39	0.74	0.92	0.69	9.49	35.00	1.37	5.23	5.76	4.64	4.43	0.05	0.21	0.56	65.00
ZAw	1.38	0.15	0.09	7.24	9.17	0.91	1.07	1.16	0.24	0.44	4.43	5.62	5.04	1.95	3.23	3.78	3.26	2.99	5.91	4.70	1.65	1.60	0.20	62.42
ARw	4.66	3.02	0.36	4.11	4.47	4.13	4.32	0.64	0.13	0.14	0.77	0.72	1.50	7.68	4.38	0.55	28.51	31.31	11.66	11.68	0.14	0.63		

Table C.7: Average dynamic connectedness in the time domain at different quantile levels over the post-outbreak period.

	BRms	BRs	CNs	ZAs	ZAcS	ARs	USs	BRc	INm	CNc	ZAwM	ZAym	ZAc	ARm	Usc	ZAw	ARw	Bsw	Usw	Uaw	CNr	Usr	INb	FROM
<i>Panel A: Lower quantile (r=0.05)</i>																								
BRms	6.26	4.99	4.02	4.34	4.32	4.64	4.81	4.63	4.67	4.62	3.88	3.69	3.93	4.88	3.92	3.99	4.18	3.99	3.88	4.26	3.73	3.75	4.60	93.74
BRs	5.80	5.42	4.03	4.31	4.08	4.86	4.77	4.68	4.38	4.07	3.90	3.77	3.92	4.98	4.02	4.02	4.27	4.05	3.99	4.27	3.94	3.81	4.67	94.58
CNs	5.35	4.64	5.50	4.47	4.24	4.75	4.50	4.68	4.39	4.22	4.02	3.95	4.01	4.81	3.59	4.15	4.27	3.95	3.73	4.20	3.92	3.81	4.82	94.50
ZAs	6.04	5.12	3.87	5.23	4.20	5.07	4.91	4.79	3.85	3.87	3.96	3.97	4.17	5.17	3.58	4.07	4.20	4.07	3.76	4.35	3.66	4.44	94.77	
ZAcS	5.20	4.55	4.20	4.60	5.16	4.40	4.55	4.53	4.70	4.48	4.16	4.03	4.33	4.79	3.76	4.15	4.25	3.86	3.74	4.35	3.91	3.67	4.62	94.84
ARs	5.59	4.71	3.99	4.43	4.12	5.77	4.69	4.69	4.52	4.59	3.97	3.79	3.97	5.10	3.70	3.89	4.32	4.08	3.79	4.11	3.93	3.79	4.45	94.23
USs	5.43	4.62	4.10	4.20	4.38	4.55	5.18	4.68	4.86	4.07	3.90	3.77	3.91	4.90	3.92	4.11	4.39	3.83	3.86	4.35	3.71	3.94	4.51	94.82
BRc	5.31	4.52	4.00	4.49	4.03	4.82	4.51	5.76	4.48	3.96	3.99	3.86	3.97	5.15	4.01	4.07	4.35	3.84	3.87	4.47	3.81	3.94	4.79	94.24
INm	5.05	4.28	4.41	4.39	4.49	4.20	4.34	4.86	5.91	4.60	4.16	4.01	4.13	4.58	3.74	4.25	4.08	3.83	3.90	4.35	3.74	3.83	4.86	94.09
CNc	5.06	4.32	4.16	4.26	4.49	4.37	4.64	4.83	5.60	4.09	3.99	4.08	4.83	3.88	4.12	4.38	3.95	3.82	4.31	3.86	3.65	4.72	94.40	
ZAwM	4.89	4.23	4.11	4.46	4.46	4.43	4.24	4.74	4.56	4.58	4.83	4.59	4.38	4.79	4.00	4.34	4.24	3.77	3.86	4.38	3.75	3.78	4.60	95.17
ZAym	5.17	4.49	3.82	4.69	4.30	4.60	4.41	4.83	3.97	4.09	4.64	4.74	4.56	5.02	3.88	4.33	4.26	4.00	3.84	4.34	3.69	3.77	4.57	95.26
ZAc	5.53	4.64	3.91	4.70	4.30	4.78	4.57	4.87	4.16	4.07	4.20	4.24	4.70	5.19	3.63	4.24	4.28	4.04	3.80	4.28	3.63	3.70	4.53	95.30
ARm	5.96	4.99	3.91	4.42	4.01	5.04	4.72	4.83	4.14	4.03	3.79	3.70	4.11	6.00	3.69	4.01	4.44	4.05	3.88	4.23	3.71	4.55	94.00	
USc	5.41	4.54	4.16	4.28	4.38	4.41	4.37	4.73	4.66	4.31	4.00	3.81	4.13	4.69	4.80	4.25	4.05	3.86	4.44	3.84	3.87	4.70	95.20	
ZAw	5.69	4.76	3.90	4.73	4.21	4.68	4.45	4.59	4.01	4.01	4.06	4.00	4.39	4.98	3.61	5.06	4.42	4.19	3.95	4.15	3.73	3.75	4.69	94.94
ARw	5.27	4.44	4.20	4.27	4.22	4.47	4.36	4.72	4.61	4.29	4.09	3.93	3.96	4.89	4.00	4.17	5.01	3.96	4.03	4.48	3.99	3.81	4.85	94.99
Bsw	5.54	4.80	3.87	4.68	4.22	4.70	4.53	4.64	4.22	3.98	3.99	3.91	4.24	4.89	3.60	4.19	4.27	4.94	4.10	4.53	3.67	3.94	4.55	95.06
Usw	5.10	4.36	4.06	4.26	4.44	4.34	4.37	4.56	4.81	4.79	4.04	3.88	4.16	4.92	3.83	4.14	4.61	4.14	4.87	4.39	3.56	3.87	4.49	95.13
Uaw	5.30	4.67	4.18	4.51	4.40	4.49	4.49	4.64	4.55	4.35	4.04	3.85	4.21	4.84	3.71	4.05	4.22	4.35	3.92	5.13	3.84	3.72	4.53	94.87
Cnr	5.33	4.51	4.10	4.42	4.49	4.59	4.37	4.61	4.74	4.68	3.97	3.81	4.04	4.73	3.62	4.11	4.17	3.88	3.80	4.22	5.16	3.90	4.77	94.84
Usr	5.25	4.41	3.98	4.40	4.09	4.66	4.34	4.99	4.48	4.20	4.14	4.01	4.00	4.81	3.80	4.22	4.39	3.94	4.02	4.24	3.82	5.10	4.71	94.90
Inb	5.11	4.37	4.20	4.29	4.36	4.53	4.33	4.74	4.72	4.20	4.12	3.95	4.03	4.78	4.16	4.33	4.55	3.91	3.90	4.35	3.99	3.86	6.23	93.77
TO	118.38	100.98	89.38	97.59	94.25	101.19	99.02	103.61	98.29	94.83	89.17	86.51	90.65	107.67	83.28	91.03	94.64	87.72	85.29	95.05	83.49	83.54	102.03	2177.64
Inc.Own	124.64	106.41	94.88	102.82	99.41	106.96	104.19	109.41	104.20	100.43	94.01	91.25	95.35	113.67	88.08	96.08	99.64	92.67	90.16	100.18	88.66	88.64	108.26	TCI
NET	24.64	6.41	-5.12	2.82	-0.59	6.96	4.19	9.41	4.20	0.43	-5.99	-8.75	-4.65	13.67	-11.92	-3.92	-0.36	-7.33	-9.84	0.18	-11.34	-11.36	8.26	94.68
NPT	22.00	16.00	7.00	15.00	11.00	16.00	15.00	18.00	14.00	10.00	5.00	5.00	11.00	20.00	2.00	10.00	13.00	6.00	3.00	11.00	1.00	2.00	20.00	
<i>Panel B: Median quantile (r=0.50)</i>																								
BRms	27.75	22.63	0.14	0.32	0.66	8.21	14.89	1.78	0.85	0.89	0.52	0.38	1.09	6.46	2.42	0.16	3.16	1.76	3.17	1.26	0.33	0.71	0.46	72.25
BRs	22.01	27.06	0.21	0.30	0.54	8.43	15.62	1.97	1.09	0.96	0.53	0.40	0.91	6.32	2.61	0.15	3.47	1.75	2.74	1.30	0.30	0.97	0.37	72.94
CNs	2.13	1.64	75.20	50.50	1.86	0.86	2.83	1.63	0.71	1.39	1.16	1.32	1.23	0.99	1.32	0.38	0.58	0.71	0.80	0.85	0.91	0.39	0.60	24.80
ZAs	7.68	8.15	0.39	23.67	8.83	5.51	6.32	3.09	0.57	1.29	6.31	6.78	7.09	3.95	0.70	2.91	1.35	1.43	1.56	1.46	0.21	0.55	21.63	
ZAcS	8.68	10.89	0.87	8.26	23.29	4.05	6.18	1.34	1.01	1.03	4.97	5.73	8.40	4.27	0.89	2.88	1.14	1.66	1.35	1.72	0.28	0.89	0.23	76.71
ARs	11.40	11.88	0.52	0.43	0.39	40.80	9.01	2.36	1.30	1.04	0.33	0.21	0.58	8.26	1.37	0.38	3.69	1.42	1.61	1.39	0.40	0.83	0.40	59.20
USs	18.06	19.38	0.43	0.27	0.90	8.00	34.02	1.18	0.88	1.10	0.61	0.36	0.20	4.55	2.43	0.27	2.02	1.15	1.91	0.70	0.55	0.76	0.28	65.98
BRc	3.35	3.42	1.01	1.04	0.85	2.66	1.78	53.93	1.34	1.34	1.95	1.97	2.71	7.66	3.29	0.72	2.78	0.68	3.79	2.04	0.52	0.88	0.29	46.07
INm	1.69	1.92	0.60	0.86	0.61	0.26	1.62	0.81	0.65	0.52	0.37	0.72	0.38	1.21	0.50	0.21	0.26	0.65	1.30	0.77	0.17	0.77	0.17	19.19
CNc	3.31	3.74	0.90	2.13	1.44	2.88	2.44	3.32	0.54	5.31	2.31	2.02	2.57	4.13	0.39	0.57	2.33	1.33	3.62	2.11	1.05	0.57	0.20	46.59
ZAwM	1.15	1.17	0.28	6.38	5.41	1.85	0.88	2.53	0.38	0.89	26.78	12.76	12.47	1.86	4.81	2.20	0.99	2.12	1.58	0.19	0.45	0.52	73.22	
ZAym	1.32	1.64	0.25	6.12	5.74	2.04	1.06	2.99	0.44	0.88	20.30	23.87	14.08	3.59	2.38	4.97	2.42	0.98	2.24	1.65	0.29	0.44	0.29	76.13
ZAc	2.62	2.86	0.31	6.29	8.06	2.44	1.35	2.65	0.44	1.28	10.72	13.82	23.89	4.76	2.19	5.97	1.92	2.05	1.97	0.29	0.59	0.23	76.11	
ARm	8.19	8.05	0.30	0.22	0.41	7.81	5.26	5.34	0.29	1.63	0.94	1.79	36.02	3.42	0.57	7.12	2.55	5.78	2.33	0.52	0.76	0.17	63.98	
USc	4.73	5.30	0.18	0.34	0.24	1.83	4.38	2.76	0.31	0.62	0.28	0.69	4.26	52.03	0.47	3.56	3.93	6.79	3.18	0.48	1.69	0.30	47.97	
ZAw	1.12	0.99	0.41	4.17	4.40	0.98	0.78	0.62	0.42	0.54	6.65	7.79	9.38	2.48	2.05	37.84	4.55	4.30	6.02	3.32	0.35	0.70	0.19	62.16
ARw	3.94	4.41	0.14	0.27	0.22	3.71	4.28	2.10	0.90	0.47	1.77	1.42	1.35	8.74	2.72	0.52	41.25	5.59	11.46	4.19	0.34	1.69	0.32	58.75
Bsw	2.80	2.84	0.28	1.01	1.12</																			

Table C.8: Average dynamic connectedness in the frequency domain at different quantile levels over the pre-outbreak period.

and second values in parentheses represent median and long term frequency connectedness measures, respectively, while all other values indicate short-term frequency connectedness. Each cell shows the spillovers from the grain listed in the top row to the grain listed in the first column. ‘FROM’ indicates the total directional return connectedness received from other grains. ‘TO’ denotes the directional return connectedness given to other grains. ‘Inc.Own’ represents the sum of the total directional connectedness of series  $i$  to all other series  $j$  and to itself. ‘NET’ is the net total directional return connectedness. ‘TCI’ reflects the overall spillover strength across the grains.

Table C.9: Average dynamic connectedness in the frequency domain at different quantile levels over the post-outbreak period.

## Appendix D. Network connectedness in the frequency domain

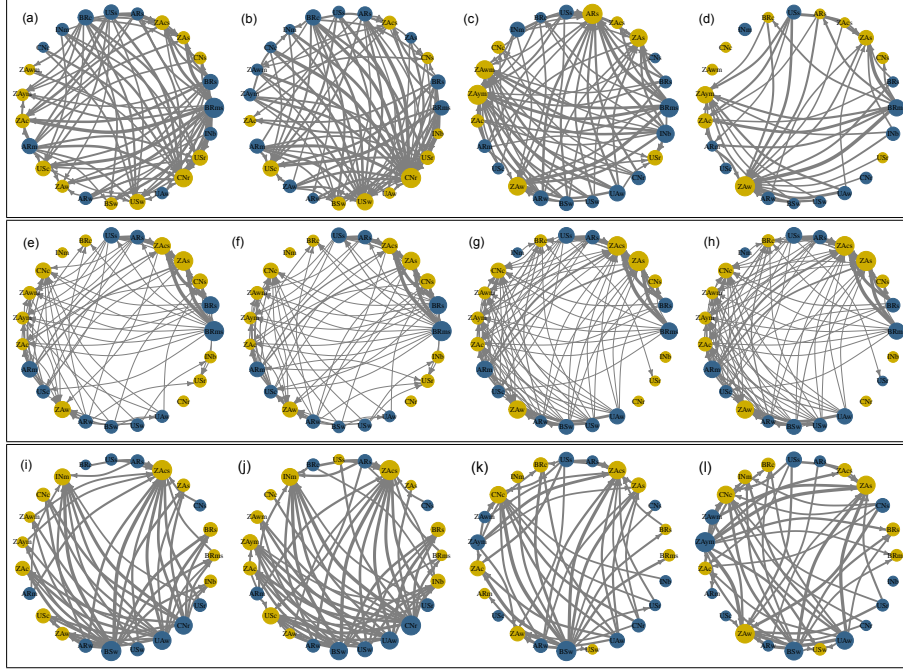


Figure D.14: Network connectedness in the frequency domain (full sample). The upper, middle, and lower panels correspond to the extreme lower ( $\tau = 0.05$ ), conditional median ( $\tau = 0.5$ ), and extreme upper ( $\tau = 0.95$ ) quantiles, respectively. Specifically, the first to the fourth columns respectively correspond to overall, short-term, medium-term, and long-term connectedness.

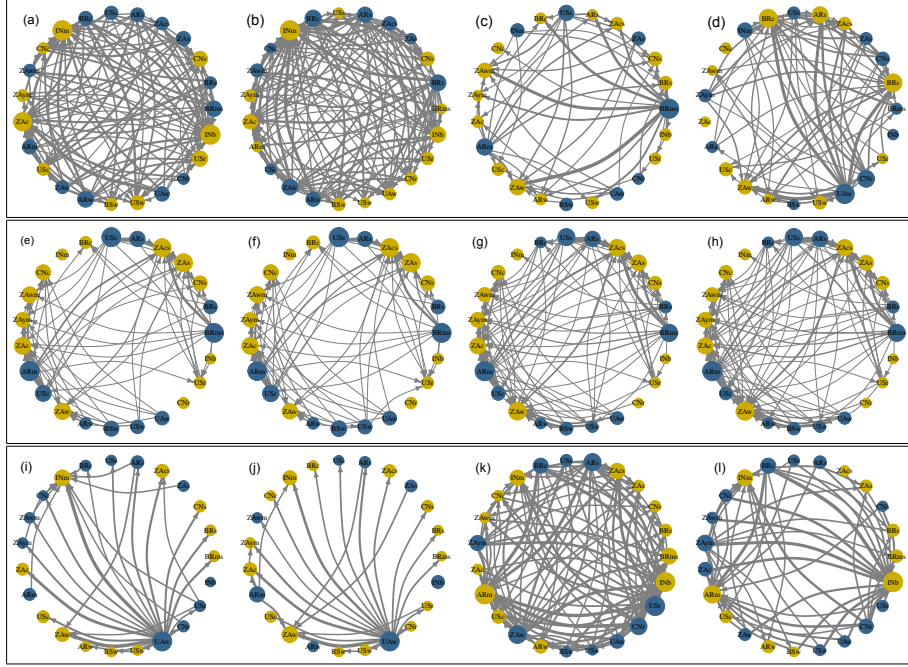


Figure D.15: Network connectedness in the frequency domain (pre-outbreak). The upper, middle, and lower panels correspond to the extreme lower ( $\tau = 0.05$ ), conditional median ( $\tau = 0.5$ ), and extreme upper ( $\tau = 0.95$ ) quantiles, respectively. Specifically, the first to the fourth columns respectively correspond to overall, short-term, medium-term, and long-term connectedness.

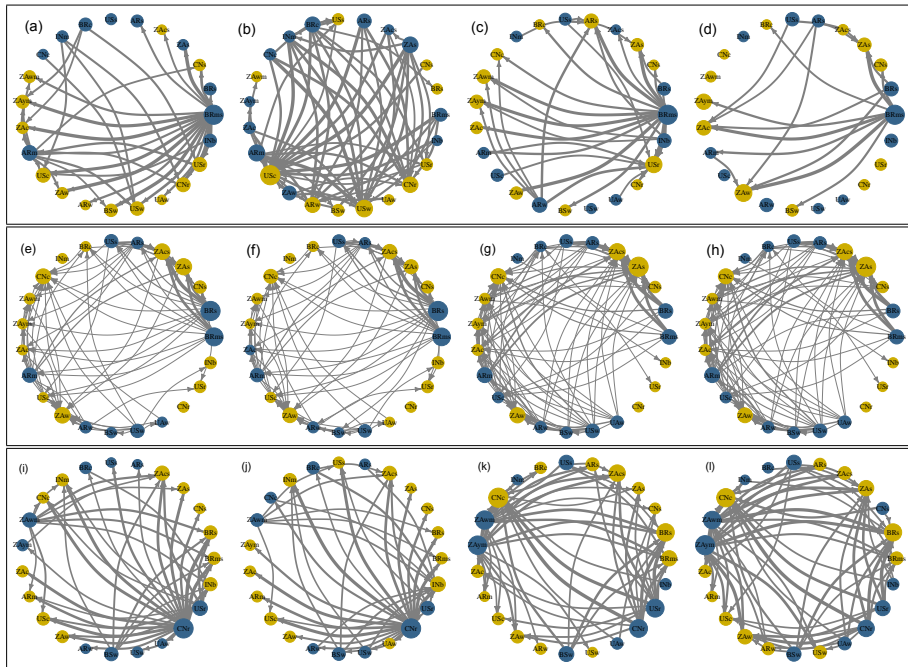


Figure D.16: Network connectedness in the frequency domain (post-outbreak). The upper, middle, and lower panels correspond to the extreme lower ( $\tau = 0.05$ ), conditional median ( $\tau = 0.5$ ), and extreme upper ( $\tau = 0.95$ ) quantiles, respectively. Specifically, the first to the fourth columns respectively correspond to overall, short-term, medium-term, and long-term connectedness.

## Appendix E. Dynamic total and net connectedness across time and quantiles in the frequency domain

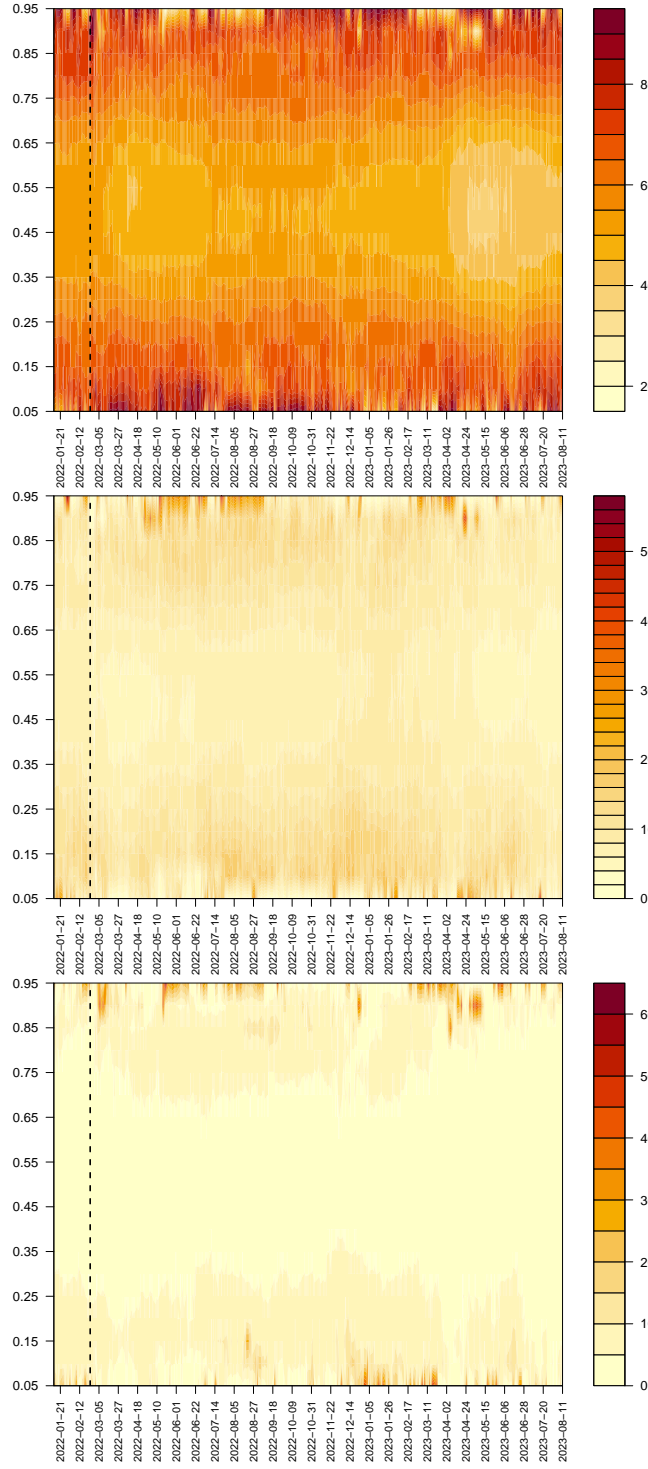


Figure E.17: The top, middle, and bottom subfigures represent the short-term, medium-term, and long-term dynamic total connectedness across time and quantiles, respectively.

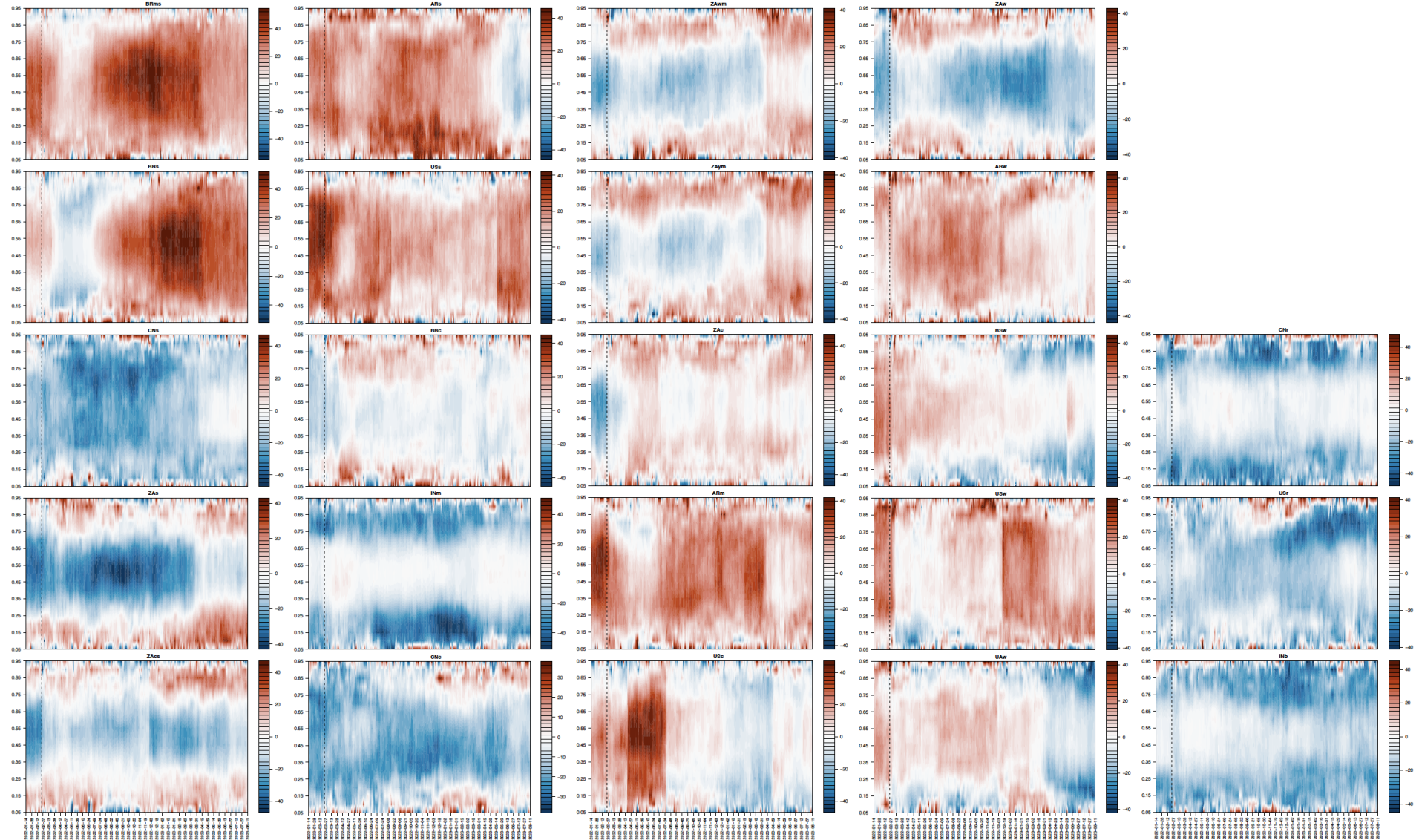


Figure E.18: Net total directional connectedness across time and quantiles in the short-term frequency domain.

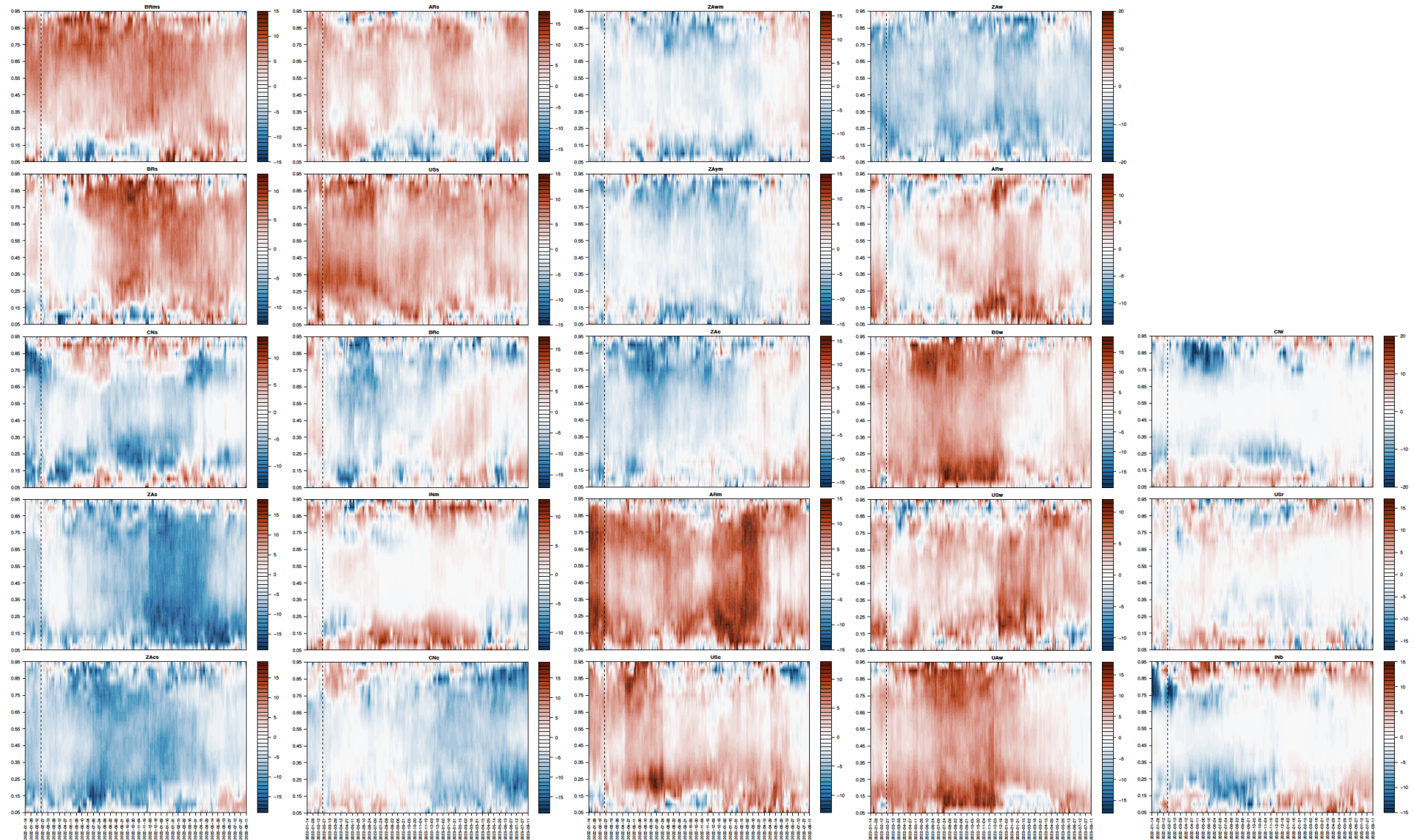


Figure E.19: Net total directional connectedness across time and quantiles in the medium-term frequency domain.

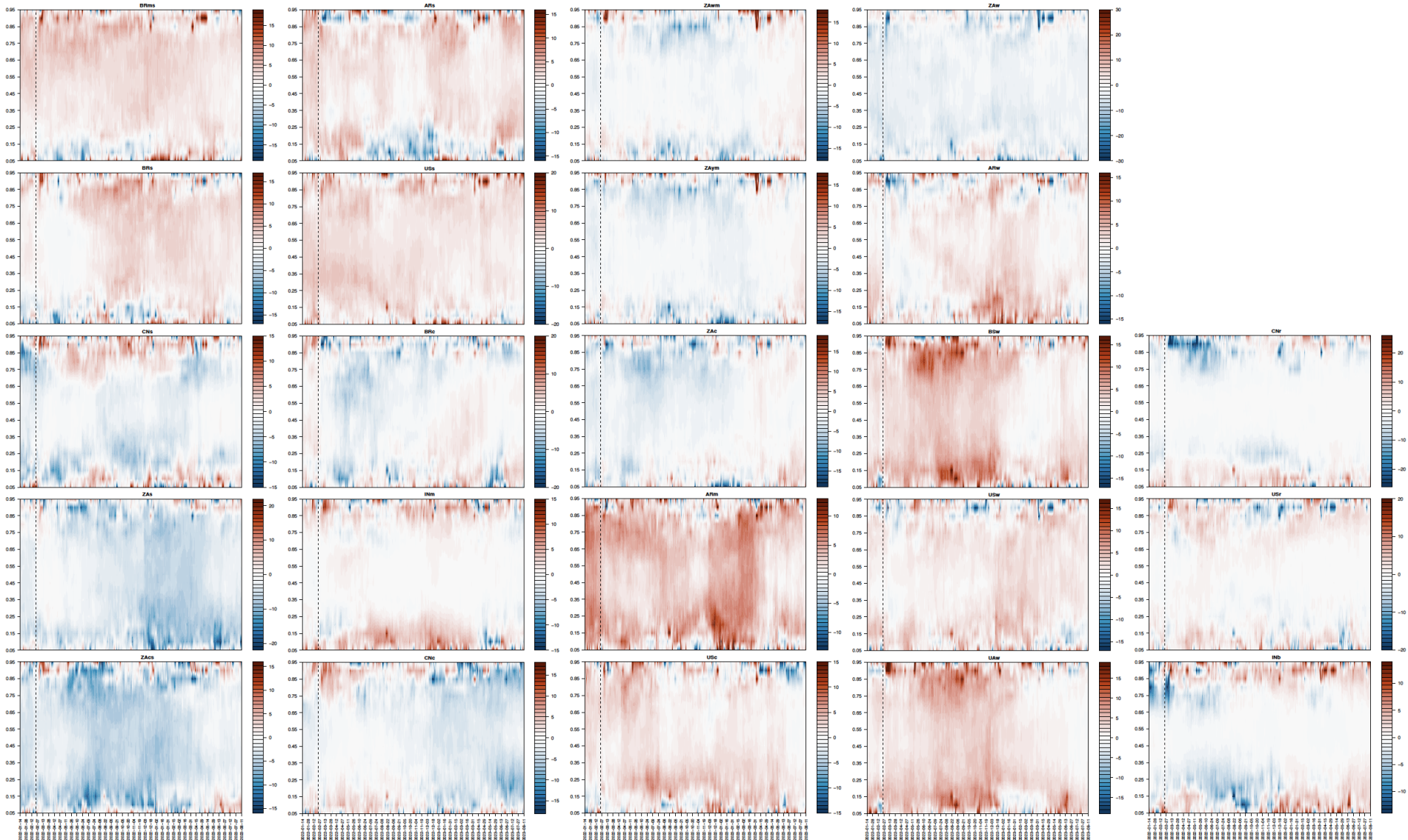


Figure E.20: Net total directional connectedness across time and quantiles in the long-term frequency domain.